

TI 设计: TIDA-01407

汽车类 400W、48V 电池输入、12V 输出电源参考设计



说明

此参考设计是一种 400W 相移全桥汽车转换器，可将 36V 至 60V 直流输入转换成 12V 输出。这种增强型相移全桥控制器实现了可编程延迟，可确保在多种操作条件下实现零电压开关 (ZVS)。输出实现了同步整流，从而可实现快速瞬态响应和高环路带宽。该系统在无负载时可提供 12V 的稳定电压，待机功耗小于 100mW。可通过变压器实现伪隔离，以防止 48V 电池短路至次级侧。半桥栅极驱动器可承受最大 120V 的直流升压电压。

资源

TIDA-01407	设计文件夹
UCC28951-Q1	产品文件夹
UCC27212-Q1	产品文件夹
UCC27511-Q1	产品文件夹



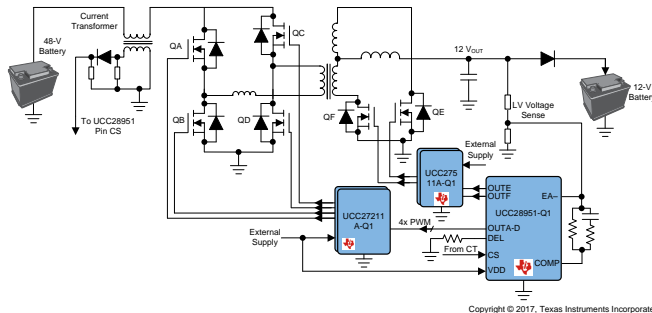
咨询我们的 E2E 专家

特性

- 相移全桥转换器可在 36V 至 60V 直流输入电压下运行，输出功率高达 400W
- 借助额外散热，输出功率可扩展至 500W，便于根据客户要求轻松定制
- 软开关，使用 UCC28951-Q1 实现相移全桥，1 级
- 可实现多相操作间的同步
- 在输入电压范围为 36V 至 60V 且无负载的条件下可提供 12V 稳压，待机功耗小于 100mW
- 通过变压器实现伪隔离；若 MOSFET 短路，则负载无法达到 48V
- 高效同步整流
- 可在整个负载范围内实现高效率的自适应延迟功能

应用

- [HEV/EV 牵引逆变器](#)
- [干式双离合变速器](#)
- [电子控制单元](#)
- [HEV/EV 直流/直流转换器](#)

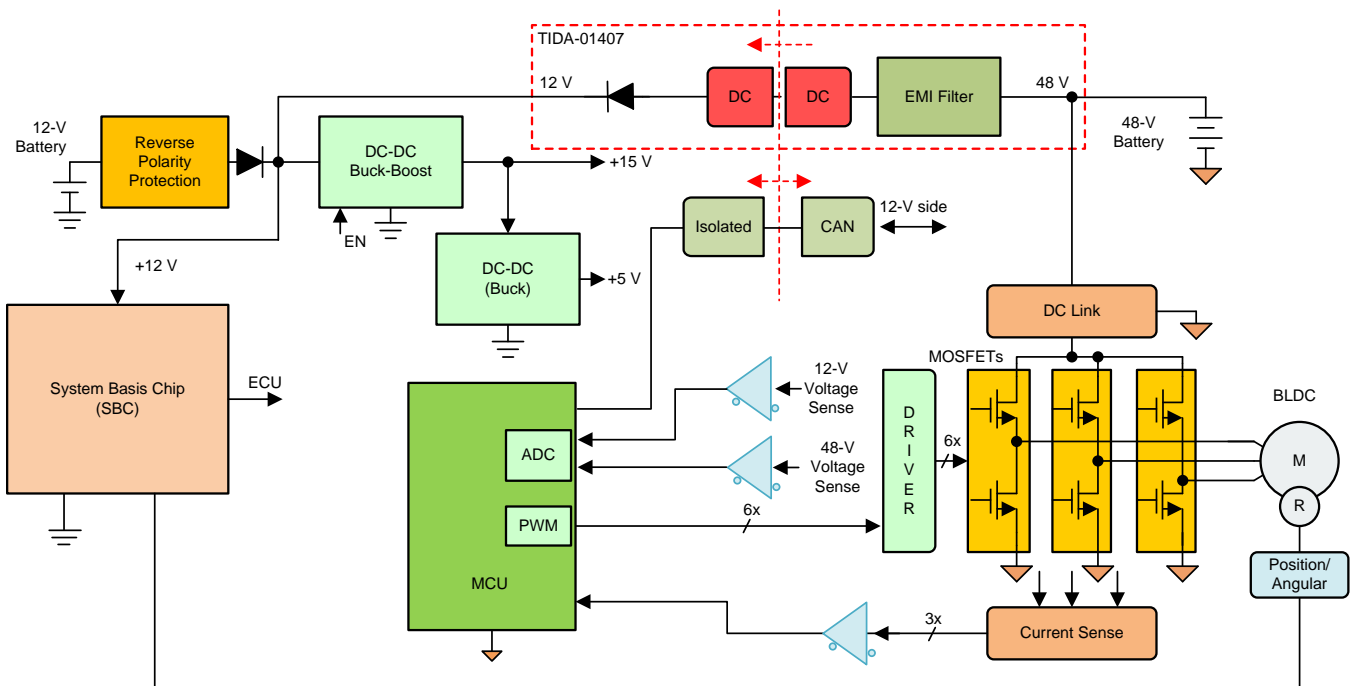


该 TI 参考设计末尾的重要声明表述了授权使用、知识产权问题和其他重要的免责声明和信息。

1 System Overview

This reference design is a 400-W DC-DC power supply that generates a 12-V rail from the 48-V car battery in a mild hybrid electric vehicle (MHEV) system. The design implements a phase-shifted full-bridge topology which is capable of delivering 400 W of output power and handling an input voltage range of 36-V to 60-V DC without losing regulation. The input voltage withstand rating can be increased by increasing the MOSFET blocking voltage for the LV148 standard compliance. The enhanced, phase-shifted full-bridge controller UCC28951-Q1 implements programmable delays which ensure zero voltage switching (ZVS) over a wide range of operating conditions. The output side implements synchronous rectification, which enables fast transient response and a high loop bandwidth. The system regulates 12 V at no load with less than 100 mW of standby power. Pseudo isolation is achieved through the use of a transformer, which means the 48V does not apply to the load if the MOSFETs are shorted. The half-bridge gate drivers, which drive the high side and low side MOSFETs together at the primary side, can withstand a maximum boot voltage of 120-V DC. The controller regulates the output voltage through the transformer primary side, which eliminates the use of an Optocoupler and leads to a higher reliability and smaller form-factor board.

图 1 shows a block diagram example of the 48-V battery-inverter-driven motor system. The TIDA-01407 serves as a redundant supply to the 12-V battery voltage rail. As the diagram shows, the isolated DC-DC (TIDA-01407) is connected to the 48-V battery side and the non-isolated DC-DC is connected to the 12-V battery side (TIDA-01179 [1]). Both designs are in ORing configuration and provide the power to the downstream loads. TIDA-01179, which includes a buck-boost converter and a buck converter, creates the front-end power for the 12-V car battery.



Copyright © 2017, Texas Instruments Incorporated

图 1. System Block Diagram of 48-V Battery-Driven Inverter and Implementation of TIDA-01407

1.1 Key System Specifications

表 1 lists the key system specifications of TIDA-01407. The design can withstand a 36-V to 60-V input voltage range without losing regulation at the output. The input voltage range can be enlarged by increasing the MOSFET size for LV148 standard compliance. The output power can be increased by adding heatsinks.

表 1. Key System Specifications

PARAMETER	SPECIFICATIONS
Input	<ul style="list-style-type: none"> • 36 V to 60 V, 48-V nominal
Output	<ul style="list-style-type: none"> • 12-V DC • 33.3-A continuous • Ripple < 3% V_{OUT} • Load step 3% to 100%; voltage deviation < 5%
Mechanics	<ul style="list-style-type: none"> • Silent power = no forced air • Efficiency > 95% • No heatsink • Slim line, maximum height < 20 mm
Extras	<ul style="list-style-type: none"> • Extendable to 500 W with heatsinking • Synchronize for multiple phase operations • No load with < 100-mW standby power • Switching frequency (\approx300 kHz) • 36-V to 60-V input without losing regulation • Pseudo isolation through transformer

2 System Description

2.1 Block Diagram

图 2 shows the system block diagram. The design consists of three main functional elements.

1. Current sensing at the primary side through the current transformer – This feature is for cycle-by-cycle overcurrent protection and adaptive delay control.
2. Power stage of the phase-shifted full-bridge at the primary side – This power stage implements the zero voltage soft-switching scheme and variable power-saving features for improving the efficiency over a wide load current range. The device can tolerate automotive electronics operating from a car battery, which experiences transient loads such as cold cranks and load dumps that can range up to 80 V and are easily scalable to 100 V.
3. Synchronous rectification MOSFETs at the secondary side – This element offers several benefits and functions to:
 - Boost the system efficiency by reducing the voltage drop over the drain-to-source
 - Reduce voltage overshoots and undershoots caused by the load steps
 - Enable fast transient response and a high loop bandwidth.

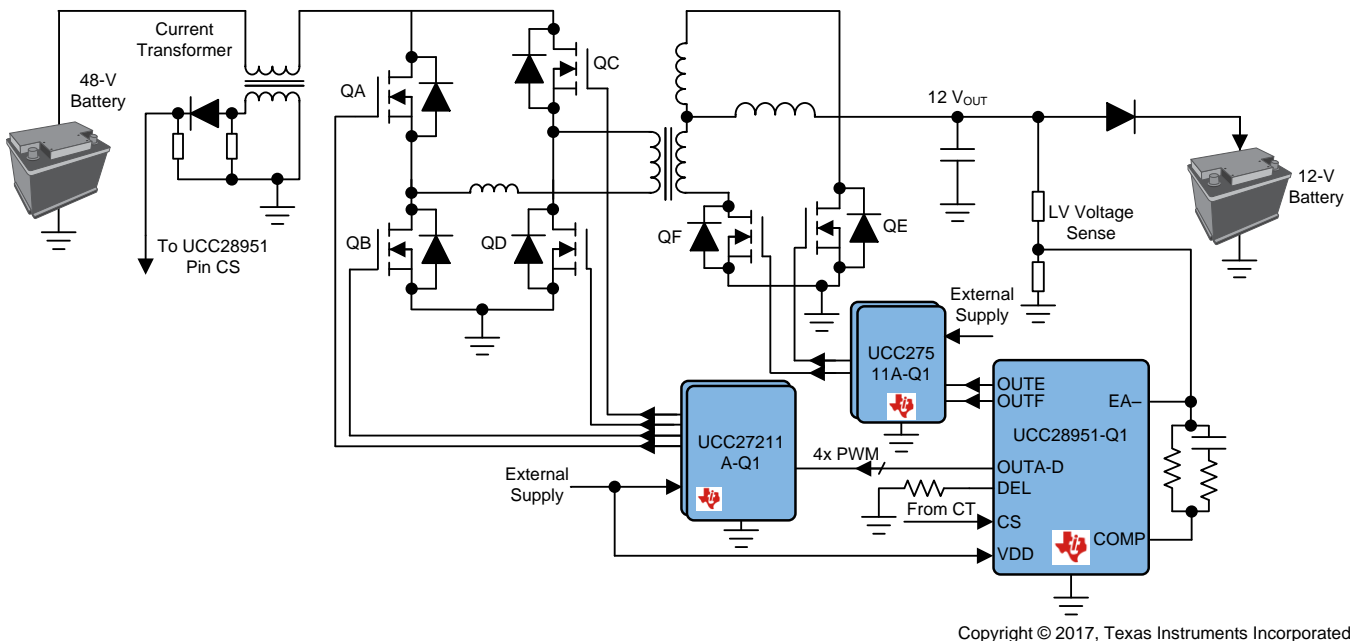


图 2. TIDA-01407 Block Diagram

2.2 Highlighted Products

The TIDA-01407 reference design features the following Texas Instruments devices.

2.2.1 UCC28951-Q1

The UCC28951-Q1 is an enhanced phase-shifted full-bridge controller which implements programmable delays to ensure ZVS operation over a wide range of operating conditions. The device contains all of the necessary features and multiple light load management to ensure maximized efficiency at overall conditions. The UCC28951-Q1 includes support for current or voltage mode control. The device features a programmable switching frequency up to 1 MHz and a wide set of protection features including cycle-by-cycle current limit, undervoltage lockout (UVLO), and thermal shutdown.

2.2.2 UCC27212-Q1

The UCC27212-Q1 device is a half-bridge driver with 120-V boot voltage and 4-A sink. The UCC27212-Q1 has a 4-A source-peak drive-current capability, which allows for driving large power MOSFETs with minimized switching losses during the transition through the Miller Plateau of the MOSFET. The switching node of the UCC27212-Q1 (HS pin) can handle –18 V maximum, which protects the high-side channel from inherent negative voltages caused by parasitic inductance and stray capacitance. An on-chip 120-V rated bootstrap diode eliminates the external discrete diodes. UVLO is provided for both the high-side and the low-side drivers, which in turn provides symmetric turnon and turnoff behavior and forces the outputs low if the drive voltage is below the specified threshold.

2.2.3 UCC27511A-Q1

The UCC27511A-Q1 device is a single-channel, low-side, high-speed gate driver with 4-A peak source and 8-A peak sink currents with asymmetrical drive, which boosts immunity against the parasitic Miller turnon effect. The UCC27511A-Q1 is capable of sourcing and sinking high peak-current pulses into capacitive loads offering rail-to-rail drive capability and extremely small propagation delay of 13 ns (typical). The device is designed to operate over a wide VDD range of 4.5 V to 18 V and a wide temperature range of –40°C to 140°C. Internal UVLO circuitry on the VDD pin holds the output low outside the VDD operating range.

2.3 System Design Theory

The TIDA-01407 TI Design implements a phase-shifted full bridge to achieve high efficiency over a wide range of operating conditions. The ZVS on the primary side of the converter reduces the switching losses and electromagnetic interference (EMI). Synchronous rectification on the secondary side is implemented to enable fast transient response and a high loop bandwidth [2].

2.3.1 Power Budget

The power budget is set as shown in [公式 1](#) to meet the efficiency goal.

$$P_{\text{BUDGET}} = P_{\text{OUT}} \times \frac{(1 - \eta)}{\eta} = 400 \text{ W} \times \frac{(1 - 94\%)}{94\%} = 25.5 \text{ W} \quad (1)$$

2.3.2 Transformer Parameter Calculations

This subsection introduces transformer parameter calculations, which include turns ratio, magnetizing inductance, leakage inductance, and so forth [3].

The transformer turns ratio is calculated in 公式 2.

$$a_1 = \frac{N_p}{N_s} \quad (2)$$

where,

- N_p is the number of turns at the transformer primary side
- N_s is the number of turns at the transformer secondary side.

The voltage drop from the BSC072N08NS5 MOSFET (V_{RDSON}) is calculated in 公式 3 as:

$$V_{RDSON} = I_{DS} \times R_{DSON} = 11.2 \text{ A} \times 7.2 \text{ m}\Omega = 0.08 \text{ V} \quad (3)$$

where,

- I_{DS} is the current flowing through the drain-to-source of the primary MOSFETs.

The maximum duty cycle (D_{MAX}) is set as 70% at the minimum specified input voltage (V_{INMIN}). The transformer turns ratio is calculated in 公式 4 as:

$$a_1 = \frac{(V_{INMIN} - 2 \times V_{RDSON}) \times D_{MAX}}{V_{OUT} + V_{RDSON}} = \frac{(36 \text{ V} - 2 \times 0.08 \text{ V}) \times 70\%}{12 \text{ V} + 0.08} = 2.07 \quad (4)$$

Set the turns ratio to the closest whole turn as $a_1 = 2.5$. The typical duty cycle (D_{TYP}) at the maximum input voltage (60 V) is calculated in 公式 5 as:

$$D_{TYP} = \frac{(V_{OUT} + V_{RDSON}) \times a_1}{(V_{IN} - 2 \times V_{RDSON})} = \frac{(12 \text{ V} + 0.08 \text{ V}) \times 2.5}{60 \text{ V} - 2 \times 0.08 \text{ V}} = 0.504 \quad (5)$$

The maximum duty cycle is recalculated again in 公式 6 with the selected turns ratio:

$$D_{MAX} = \frac{a_1 \times (V_{OUT} + V_{RDSON})}{V_{INMIN} - 2 \times V_{RDSON}} = \frac{2.5 \times (12 \text{ V} + 0.08 \text{ V})}{36 \text{ V} - 2 \times 0.08 \text{ V}} = 0.84 \quad (6)$$

The output inductor ripple current ($\Delta I_{L_{OUT}}$) is calculated in 公式 7 as:

$$\Delta I_{L_{OUT}} = \frac{P_{OUT} \times 0.2}{V_{OUT}} = \frac{400 \text{ W} \times 0.2}{12} = 6.7 \text{ A} \quad (7)$$

The magnetizing inductance (L_{MAG}) of the primary of the transformer (T1) must be sufficient to ensure that the converter operates in peak current-mode control. A small L_{MAG} results in a large magnetizing current, which causes the converter to operate in voltage mode instead. L_{MAG} is calculated in 公式 8 at the maximum input voltage

$$L_{MAG} \geq \frac{V_{IN_MAX} \times (1 - D_{TYP})}{\frac{\Delta I_{OUT} \times 0.5}{a_1} \times F_{SW}} = \frac{60 \text{ V} \times (1 - 0.504)}{\frac{6.7 \text{ A} \times 0.5}{2.5}} = 74 \mu\text{H} \quad (8)$$

where,

- F_{SW} is the switching frequency of the converter.

L_{MAG} is selected as 80 μH .

图 3 shows the primary ($I_{PRIMARY}$) and secondary side currents flowing through the transformer (I_{QE} and I_{QF}). I_{QE} and I_{QF} are also the currents that flow through the synchronous rectifiers. Calculations of the current values are provided in the following equations.

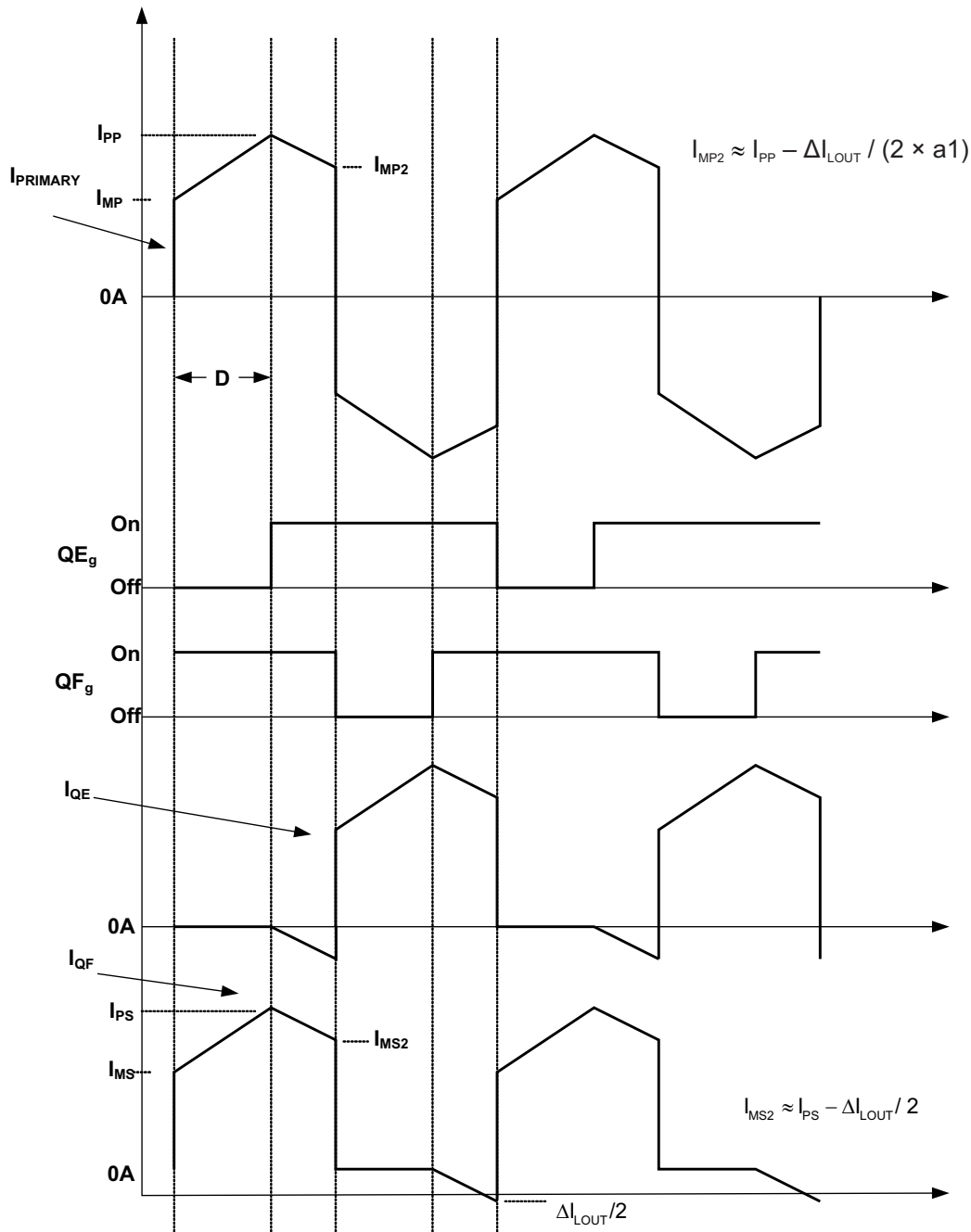


图 3. Transformer Primary Side and Secondary Side Currents

The peak current (I_{PS}) and the minimum current (I_{MS}) of the transformer secondary side are calculated in 公式 9, 公式 10, and 公式 11 as:

$$I_{PS} = \frac{P_{OUT}}{V_{OUT}} + \frac{\Delta I_{LOUT}}{2} = \frac{400}{12} + \frac{6.7 \text{ A}}{2} = 36.7 \text{ A} \quad (9)$$

$$I_{MS} = \frac{P_{OUT}}{V_{OUT}} - \frac{\Delta I_{LOUT}}{2} = \frac{400}{12} - \frac{6.7 \text{ A}}{2} = 30 \text{ A} \quad (10)$$

$$I_{MS2} = I_{PS} - \frac{\Delta I_{LOUT}}{2} = 36.7 \text{ A} - \frac{6.7 \text{ A}}{2} = 33.35 \text{ A} \quad (11)$$

The secondary RMS current (I_{SRMS1}) when the energy is being delivered to the secondary is calculated in 公式 12:

$$\begin{aligned}
 I_{SRMS1} &= \sqrt{\left(\frac{D_{MAX}}{2}\right) \times \left(I_{PS} \times I_{MS} + \frac{(I_{PS} - I_{MS})^2}{3}\right)} \\
 &= \sqrt{\left(\frac{70\%}{2}\right) \times \left(36.7 \text{ A} \times 30 \text{ A} + \frac{(36.7 \text{ A} - 30 \text{ A})^2}{3}\right)} \\
 &= 19.8 \text{ A}
 \end{aligned} \tag{12}$$

The secondary RMS current (I_{SRMS2}) when the current is circulating through the transformer while MOSFETs Q1, Q4, Q5, Q6, A7, and Q8 are all ON is calculated in 公式 13 as:

$$\begin{aligned}
 I_{SRMS2} &= \sqrt{\left(\frac{1 - D_{MAX}}{2}\right) \times \left(I_{PS} \times I_{MS2} + \frac{(I_{PS} - I_{MS2})^2}{3}\right)} \\
 &= \sqrt{\left(\frac{1 - 70\%}{2}\right) \times \left(36.7 \text{ A} \times 33.35 \text{ A} + \frac{(36.7 \text{ A} - 33.35 \text{ A})^2}{3}\right)} \\
 &= 13.6 \text{ A}
 \end{aligned} \tag{13}$$

The secondary RMS current (I_{SRMS3}) caused by the negative current in the opposing winding during the freewheeling period is calculated in 公式 14 as:

$$I_{SRMS3} = \frac{\Delta I_{LOUT}}{2} \times \sqrt{\left(\frac{1 - D_{MAX}}{2 \times 3}\right)} = \frac{6.7 \text{ A}}{2} \times \sqrt{\left(\frac{1 - 70\%}{2 \times 3}\right)} = 0.75 \text{ A} \tag{14}$$

As a result, the total RMS current that flows into the transformer secondary (I_{SRMS}) is calculated in 公式 15 as:

$$I_{SRMS} = \sqrt{I_{SRMS1}^2 + I_{SRMS2}^2 + I_{SRMS3}^2} = \sqrt{19.8 \text{ A}^2 + 13.6 \text{ A}^2 + 0.75 \text{ A}^2} = 24 \text{ A} \tag{15}$$

The input inductor ripple current (ΔI_{LMAG}) is calculated in 公式 16 as:

$$\Delta I_{LMAG} = \frac{V_{INMIN} \times D_{MAX}}{L_{MAG} \times F_{SW}} = \frac{36 \text{ V} \times 70\%}{80 \mu\text{H} \times 300 \text{ kHz}} = 1.1 \text{ A} \tag{16}$$

The peak current that flows into the transformer primary side (I_{PP}) is calculated in 公式 17 as:

$$\begin{aligned}
 I_{PP} &= \left(\frac{P_{OUT}}{V_{OUT} \times \eta} + \frac{\Delta I_{LOUT}}{2}\right) \times \frac{1}{a_1} + \Delta I_{LMAG} \\
 &= \left(\frac{400 \text{ W}}{12 \times 93\%} + \frac{6.7 \text{ A}}{2}\right) \times \frac{1}{2.5} + 1.1 \text{ A} \\
 &= 16.8 \text{ A}
 \end{aligned} \tag{17}$$

The minimum current that flows into the transformer primary side (I_{MP}) is calculated in 公式 18 as:

$$\begin{aligned} I_{MP} &= \left(\frac{P_{OUT}}{V_{OUT} \times \eta} + \frac{\Delta I_{OUT}}{2} \right) \times \frac{1}{a_1} - \Delta I_{LMAG} \\ &= \left(\frac{400 \text{ W}}{12 \times 93\%} + \frac{6.7 \text{ A}}{2} \right) \times \frac{1}{2.5} - 1.1 \text{ A} \\ &= 14.57 \text{ A} \end{aligned} \quad (18)$$

公式 19 calculates the minimum current at the primary (I_{MP2}) when the converter primary-side switches are freewheeling.

$$\begin{aligned} I_{MP2} &= I_{PP} - \left(\frac{\Delta I_{L_{OUT}}}{2} \right) \times \frac{1}{a_1} \\ &= 16.8 \text{ A} - \frac{6.7 \text{ A}}{2} \times \frac{1}{2.5} \\ &= 15.46 \text{ A} \end{aligned} \quad (19)$$

The RMS current (I_{PRMS1}) at the transformer primary when energy is being delivered to the secondary is calculated in 公式 20 as:

$$\begin{aligned} I_{PRMS1} &= \sqrt{D_{MAX} \times \left(I_{PP} \times I_{MP} + \frac{(I_{PP} - I_{MP})^2}{3} \right)} \\ &= \sqrt{70\% \times \left(16.8 \text{ A} \times 14.6 \text{ A} + \frac{(16.8 \text{ A} - 14.6 \text{ A})^2}{3} \right)} \\ &= 13.2 \text{ A} \end{aligned} \quad (20)$$

The RMS current at the transformer primary side (I_{PRMS2}) when the converter is freewheeling is calculated in 公式 21 as:

$$\begin{aligned} I_{PRMS2} &= \sqrt{(1 - D_{MAX}) \times \left(I_{PP} \times I_{MP2} + \frac{(I_{PP} - I_{MP2})^2}{3} \right)} \\ &= \sqrt{(1 - 70\%) \times \left(16.8 \text{ A} \times 15.46 \text{ A} + \frac{(16.8 \text{ A} - 15.46 \text{ A})^2}{3} \right)} \\ &= 8.9 \text{ A} \end{aligned} \quad (21)$$

The total RMS current flowing through the transformer primary side (I_{PRMS}) is calculated in 公式 22 as:

$$I_{PRMS} = \sqrt{I_{PRMS1}^2 + I_{PRMS2}^2} = \sqrt{13.2 \text{ A}^2 + 8.9 \text{ A}^2} = 16 \text{ A} \quad (22)$$

2.3.3 Power Stage MOSFET Selection

The MOSFET selection is important to meet the system efficiency and electric safety. The breakdown voltage is selected based on the LV148 standard and the gate charge is minimized for system efficiency. BSC072N08NS5 80-V (V_{DS}), 74-A MOSFETs with 24-nC gate charges (Q_g) are selected for this design. The drain-to-source on-resistance $R_{ds(on)}$ is 7.2 m Ω . The output capacitance (C_{OSS_SPEC}) is 280 pF measured under $V_{DS} = 40 \text{ V}$ according to the data sheet.

The average output capacitance $C_{OSS_QA_AVG}$ is calculated in 公式 23 as:

$$C_{OSS_QA_AVG} = C_{OSS_SPEC} \times \sqrt{\frac{V_{DS}}{V_{INMAX}}} = 280 \text{ pF} \times \sqrt{\frac{40 \text{ V}}{60 \text{ V}}} = 229 \text{ pF} \quad (23)$$

The applied gate voltage is $V_g = 10\text{ V}$. The losses of one MOSFET are calculated in 公式 24 as:

$$\begin{aligned}
 P_Q &= I_{\text{PRMS}}^2 \times R_{\text{ds(on)}} + 2 Q_g \times V_g \times \frac{F_{\text{SW}}}{2} \\
 &= 16\text{ A}^2 \times 7.2\text{ m}\Omega + 2 \times 24\text{ nC} \times 10\text{ V} \times \frac{300\text{ kHz}}{2} \\
 &= 1.9\text{ W}
 \end{aligned}
 \tag{24}$$

2.3.4 Shim Inductor

The transformer primary side requires a certain value of inductance to be equivalently in series and achieve the ZVS. This type of inductance is called shim inductance (L_s). This inductance can be obtained either from the transformer leakage inductance or from an externally-added series inductor. The value is calculated based on the amount of energy required by the resonance. This inductance must be able to deplete the energy from the parasitic capacitance at the switch node. The parasitic capacitance is the sum of the output capacitance of the MOSFET, transformer winding capacitance, and the capacitance from the PCB layout.

The shim inductance (L_s) is calculated in 公式 25 as:

$$\begin{aligned}
 L_s &\geq \left(2 \times C_{\text{OSS_QA_AVG}}\right) \times \frac{V_{\text{INMAX}}^2}{\left(\frac{I_{\text{PP}}}{2} - \frac{\Delta I_{\text{LOUT}}}{2 \times a_1}\right)^2} \\
 &= (2 \times 229\text{ pF}) \times \frac{60\text{ V}^2}{\left(\frac{16.8\text{ A}}{2} - \frac{6.7\text{ A}}{2 \times 2.5}\right)^2} \\
 &= 0.033\text{ }\mu\text{H}
 \end{aligned}
 \tag{25}$$

This value is attainable through the transformer leakage inductance. Additionally, a 170-nH external shim inductor is added in series with the transformer primary winding to compensate the effect of circuit parasitics. 表 2 summarizes the calculated specifications of the designed transformer.

表 2. Phase-Shifted Full-Bridge Transformer Specifications

PARAMETER	SPECIFICATIONS
Power rating	$\geq 400\text{ W}$
Input voltage	36 V to 60 V
Frequency	300 kHz
Maximum duty cycle	70%
primary side inductance	$80\text{ }\mu\text{H} \pm 10\%$ at 300 KHz
Leakage inductance	0.06 μH
Output voltage	12 V
Output average current	33.3 A
Turns ratio (primary to secondary)	2.5:1
Peak current (primary)	16.8 A
Peak current (secondary)	36.7 A
RMS current (primary)	16 A
RMS current (secondary)	24 A

TI recommends the planar transformer 59023 from Payton Planar Magnetics LTD for this reference design.

2.3.5 Output Inductor Selection

The output inductor is designed for obtaining the 20% ripple current ($\Delta I_{L_{OUT}}$) at the output. The ripple current is calculated in 公式 26 as:

$$\Delta I_{L_{OUT}} = \frac{P_{OUT} \times 0.2}{V_{OUT}} = \frac{400 \text{ W} \times 0.2}{12 \text{ V}} = 6.7 \text{ A} \quad (26)$$

The required inductance (L_{OUT}) is calculated in 公式 27 as:

$$L_{OUT} = \frac{V_{OUT} \times (1 - D_{TYP})}{\Delta I_{L_{OUT}} \times F_{SW}} = \frac{12 \text{ V} \times (1 - 65\%)}{6.7 \text{ A} \times 300 \text{ kHz}} = 2.1 \mu\text{H} \quad (27)$$

The RMS current of the output inductor ($I_{L_{OUT_RMS}}$) is calculated in 公式 28 as:

$$I_{L_{OUT_RMS}} = \sqrt{\left(\frac{P_{OUT}}{V_{OUT}}\right)^2 + \left(\frac{\Delta I_{L_{OUT}}}{\sqrt{3}}\right)^2} = \sqrt{\left(\frac{400 \text{ W}}{12 \text{ V}}\right)^2 + \left(\frac{6.7 \text{ A}}{\sqrt{3}}\right)^2} = 33.6 \text{ A} \quad (28)$$

2.3.6 Output Capacitor Selection

The output capacitor is selected based on the required transient deviation with regards to a step change of the load current. A monolithic ceramic capacitor with a low equivalent series resistance (ESR) of 0.3 m Ω is selected. As a general rule, the bandwidth of the converter is estimated as shown in the following 公式 29:

$$f_{bw} = \frac{1}{10} \times F_{SW} = 30 \text{ kHz} \quad (29)$$

The output voltage deviation (ΔV_{OUT}) is targeted as shown in 公式 30:

$$\Delta V_{OUT} = V_{OUT} \times 3\% = 0.36 \text{ V} \quad (30)$$

The load step ($\Delta I_{loadstep}$) is considered to be the change from the maximum output current to zero. 15 ceramic capacitors are connected in parallel to minimize the ESR. As a result, the minimum required output capacitance is calculated in 公式 31 as:

$$C_{out_min} = \frac{1}{2\pi \times f_{bw}} \times \frac{1}{\frac{\Delta V_{OUT}}{\Delta I_{loadstep}} - ESR_{Cout}} = \frac{1}{2\pi \times 30 \text{ kHz}} \times \frac{1}{\frac{0.36 \text{ V}}{33.3 \text{ A}} - \frac{0.3 \text{ m}\Omega}{15}} = 246 \mu\text{F} \quad (31)$$

A total of 16 22- μF , 25-V X7R ceramic capacitors from Murata are selected and connected in parallel with an ESR of 0.3 m Ω .

2.3.7 Selection of Synchronous MOSFETs

Three MOSFETs are paralleled at the secondary side for each current freewheeling cycle to share the current and minimize the losses. To meet the power requirements, the 80-V, 100-A BSC057N08NS3 MOSFET from Infineon has been selected for synchronous rectification at the secondary side. 公式 32 and 公式 33 show the parameters of the MOSFET:

$$Q_{gs} = 13 \text{ nC} \quad (32)$$

$$R_{DS(on)} = 5.7 \text{ m}\Omega \quad (33)$$

The average output capacitance (C_{OSS_AVG}) is calculated based on the data sheet parameters for C_{OSS} , the drain-to-source voltage where C_{OSS_SPEC} is measured (V_{ds_SPEC}), and the maximum drain-to-source voltage in the design (V_{dsQE}) that is eventually applied to the MOSFET in the circuit. 公式 34 calculates the voltage across the MOSFET when switched off:

$$V_{dsQE} = \frac{V_{INMAX}}{a_1} = \frac{80\text{ V}}{2.5} = 32\text{ V} \quad (34)$$

公式 35 is the voltage where MOSFET C_{OSS} is specified and tested in the data sheet.

$$V_{ds_spec} = 40\text{ V} \quad (35)$$

公式 36 is the output capacitance of the selected MOSFET.

$$C_{oss_spec} = 780\text{ pF} \quad (36)$$

The average output capacitance is calculated in 公式 37 as:

$$C_{oss_avg} = C_{oss_spec} \times \sqrt{\frac{V_{dsQE}}{V_{ds_spec}}} = 780\text{ pF} \times \sqrt{\frac{32\text{ V}}{40\text{ V}}} = 0.7\text{ nF} \quad (37)$$

公式 38 is the RMS current that flows into the MOSFETs.

$$I_{QE_RMS} = I_{SRMS} = 24\text{ A} \quad (38)$$

The MOSFET data sheet provides the typical gate charge curve (see 图 4). The gate charge at the beginning of the Miller plateau is determined in 公式 39 as:

$$QE_{MILLER_MIN} = 16\text{ nC} \quad (39)$$

The gate charge at the end of the Miller plateau is determined in 公式 40 as:

$$QE_{MILLER_max} = 25\text{ nC} \quad (40)$$

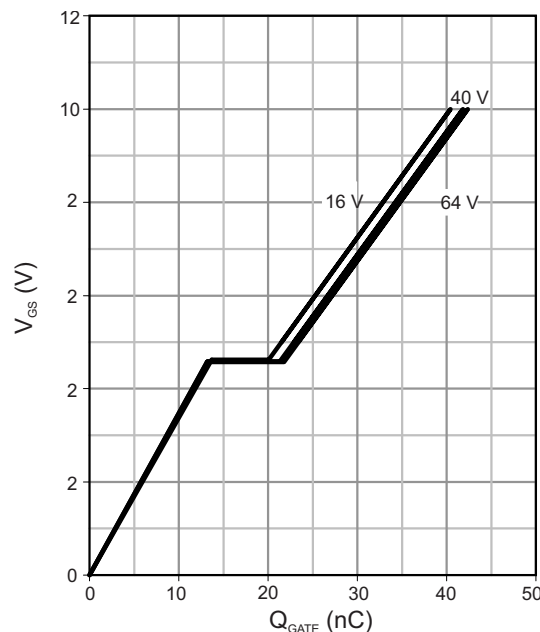


图 4. Gate Charge Curve of BSC057N08NS3

公式 41 lists the gate driver (UCC27511A-Q1) peak source current:

$$I_P = 8\text{ A} \quad (41)$$

Therefore, the MOSFET switching rise and fall times are estimated in [公式 42](#) as:

$$t_r \approx t_f = \frac{Q_{E_{\text{MILLER_max}}} - Q_{E_{\text{MILLER_min}}}}{\frac{I_P}{2}} = \frac{25 \text{ nC} - 16 \text{ nC}}{\frac{8 \text{ A}}{2}} = 2.3 \text{ ns} \quad (42)$$

Therefore, the total losses of the MOSFETs are calculated in 公式 43 as:

$$\begin{aligned}
 P_{QE} &= I_{QE_RMS}^2 \times R_{ds(on)} + \frac{P_{OUT}}{V_{OUT}} \times V_{dsQE} \times (t_r + t_f) \times \frac{F_{SW}}{2} + 2 \times C_{oss_avg} \times V_{dsQE}^2 \times \frac{F_{SW}}{2} + 2 \times Q_{gs} \times V_{gQE} \times \frac{F_{SW}}{2} \\
 &= 24 \text{ A}^2 \times 5.7 \text{ m}\Omega + \frac{400 \text{ W}}{12} \times 32 \text{ V} \times (2.3 \text{ ns} + 2.3 \text{ ns}) \times \frac{300 \text{ kHz}}{2} \\
 &= 2 \times 700 \text{ pF} \times 32 \text{ V}^2 \times \frac{300 \text{ kHz}}{2} + 2 \times 13 \text{ nC} \times 10 \text{ V} \times \frac{300 \text{ kHz}}{2} \\
 &= 3.28 \text{ W} + 4.9 \text{ mW} + 0.22 \text{ W} + 0.04 \text{ W} \\
 &= 3.55 \text{ W}
 \end{aligned}
 \tag{43}$$

2.3.8 Input Capacitor Selection

The input capacitance is selected according to the holdup and ripple current requirements. The resonant tank frequency of the transformer is calculated in 公式 44 as:

$$f_R \frac{1}{2 \times \pi \times \sqrt{L_S \times (2 \times C_{oss_QA_AVG})}} = \frac{1}{2 \times \pi \times \sqrt{0.33 \mu\text{H} \times (2 \times 324 \text{ pF})}} = 11 \text{ MHz}
 \tag{44}$$

The time delay is defined in 公式 45 as:

$$t_{DELAY} = \frac{2}{f_R \times 4} = \frac{2}{11 \text{ MHz} \times 4} = 46 \text{ ns}
 \tag{45}$$

The effective duty cycle clamp (D_{clamp}) is calculated in 公式 46 as:

$$D_{clamp} = \left(\frac{1}{F_{SW}} - t_{DELAY} \right) \times F_{SW} = \left(\frac{1}{300 \text{ kHz}} - 46 \text{ ns} \right) \times 300 \text{ kHz} = 98\%
 \tag{46}$$

The capacitance must maintain the output regulation while the input voltage reaches the minimum (V_{drop}), which 公式 47 shows:

$$V_{drop} = 20 \text{ V}
 \tag{47}$$

The input capacitance is calculated in 公式 48 based on the holdup time of 150 μs :

$$C_{IN} \geq \frac{2 \times P_{OUT} \times 150 \mu\text{s}}{(V_{IN}^2 - V_{drop}^2)} = \frac{2 \times 400 \text{ W} \times 150 \mu\text{s}}{(36 \text{ V}^2 - 20 \text{ V}^2)} = 134 \mu\text{F}
 \tag{48}$$

The high frequency RMS current delivered from the input capacitor is calculated in 公式 49 as:

$$I_{CINRMS} = \sqrt{I_{PRMS1}^2 - \left(\frac{P_{OUT}}{V_{INMIN} \times a_1} \right)^2} = \sqrt{13.2 \text{ A}^2 - \left(\frac{400 \text{ W}}{36 \text{ V} \times 2.5} \right)^2} = 13.2 \text{ A}
 \tag{49}$$

The input capacitors must be selected such that the total RMS current withstand rate is higher than 13.2 A.

2.3.9 Configuration of UCC28951-Q1

The UCC28951-Q1 phase-shifted full-bridge controller must be configured properly to ensure the system works correctly and reliably. 图 5 shows the components surrounding the controller.

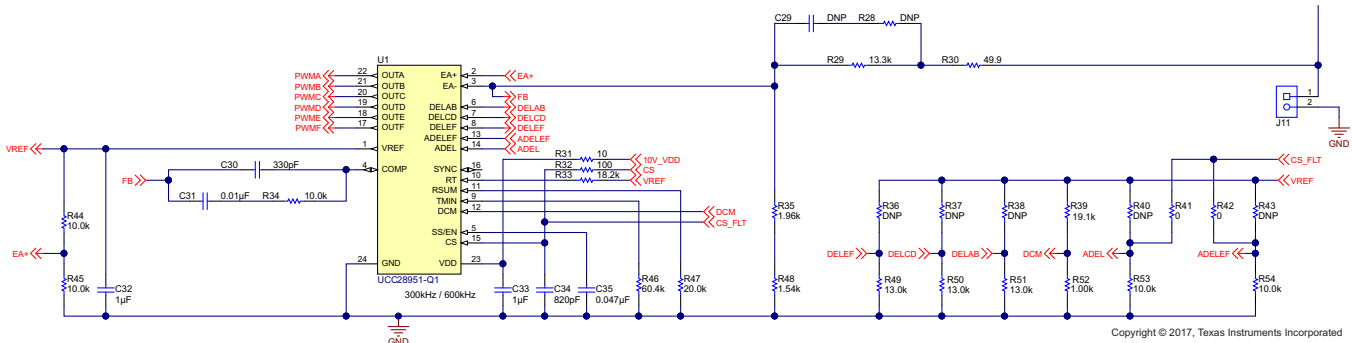


图 5. UCC28951 Configuration

2.3.9.1 Current Sense Network

The current sense network must be designed such that it has strong noise immunity to avoid it being injected into the adaptive delay circuit, which causes faulty PWM driving signals.

The nominal peak current (I_{P1}) that flows at the minimum input voltage V_{INMIN} is calculated in 公式 50 as:

$$I_{P1} = \left(\frac{P_{OUT}}{V_{OUT} \times \eta} + \frac{\Delta I_{L,OUT}}{2} \right) \times \frac{1}{a_1} + \frac{V_{INMAX} \times D_{MAX}}{L_{MAG} \times F_{SW}}$$

$$= \left(\frac{400}{12 \times 93\%} + \frac{6.7 \text{ A}}{2} \right) \times \frac{1}{2.5} + \frac{60 \times 70\%}{80 \mu\text{H} \times 300 \text{ kHz}}$$

$$= 17.5 \text{ A} \tag{50}$$

Therefore, the current transformer (T1) for this design must have the current rating higher than the 17.5 A. A current transformer from Pulse Electronics (part number PA1005.100NL) has been selected for this design. The current-sensing frequency range is from 50 kHz to 1 MHz with a turns ratio of 100:1 (see 公式 51).

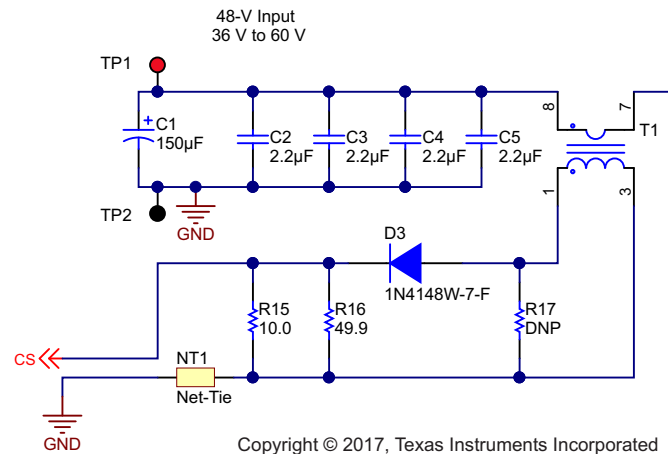
$$a_2 = \frac{I_P}{I_S} = 100 \tag{51}$$

图 6 shows a schematic of the current transformer. The cycle-by-cycle current-limit threshold of the CS pin is $V_p = 2 \text{ V}$. With 200 mV of headroom left for slope compensation, the current sense resistor (R15 in parallel with R16) is calculated in 公式 52 as:

$$R_S = \frac{V_p - 0.2 \text{ V}}{\frac{I_{P1}}{a_2} \times 1.1} = \frac{2 \text{ V} - 0.2 \text{ V}}{\frac{13.2 \text{ A}}{100} \times 1.1} = 9.4 \Omega \tag{52}$$

R_S is selected as one 10-Ω resistor and one 49.9-Ω resistor placed in parallel, which results in 8.3 Ω total. 公式 53 calculates the power losses for the R_S :

$$P_{RS} = \left(\frac{I_{PRMS1}}{a_2} \right)^2 \times R_S = \left(\frac{13.2 \text{ A}}{100} \right)^2 \times 8.3 \Omega = 0.15 \text{ W} \tag{53}$$



Copyright © 2017, Texas Instruments Incorporated

图 6. Current Sense Network

The maximum voltage across D3 (V_{DA}) is calculated in 公式 54 as:

$$V_{DA} = V_P \times \frac{D_{CLAMP}}{1 - D_{CLAMP}} = 2 \times \frac{98\%}{1 - 98\%} = 98 \text{ V} \quad (54)$$

This design uses a fast reverse-recovery diode (part number 1N4148W) with 100 V of breakdown voltage.

The power loss (P_{DA}) for D3 is calculated in 公式 55 as:

$$P_{DA} = \frac{P_{OUT} \times 1.3 \text{ V}}{V_{INMIN} \times 93\% \times a_2} = \frac{400 \text{ W} \times 1.3 \text{ V}}{36 \text{ V} \times 93\% \times 100} = 0.16 \text{ W} \quad (55)$$

The reset resistor R17 is placed to demagnetize the current transformer. The buildup voltage during the ON time of the current transformer is calculated in 公式 56 as:

$$V_{T1ON} = V_f + \left(\frac{I_{PRMS1}}{a_2} \right) \times R_S = 1.3 \text{ V} + \left(\frac{13.2 \text{ A}}{100} \right) \times 10 \Omega = 2.62 \text{ V} \quad (56)$$

The buildup voltage during the OFF time of the current transformer is calculated in 公式 57 as:

$$V_{T1OFF} = \left(\frac{I_{PRMS2}}{a_2} \right) \times R_{17} = \left(\frac{8.9 \text{ A}}{100} \right) \times R_{17} \quad (57)$$

公式 58 and Equation 公式 59 are used to calculate R17 as 1.45 kΩ:

$$V_{T1ON} \times T_{1ON} = V_{T1OFF} \times T_{1OFF} \quad (58)$$

$$\frac{T_{1ON}}{T_{1OFF}} = \frac{D_{MAX}}{1 - D_{MAX}} \quad (59)$$

Resistor R32 and capacitor C34 form a low-pass filter for the current sense signal pin 15 with 公式 60 calculating a cutoff frequency of:

$$f_L = \frac{1}{2 \times \pi \times R_{32} \times C_{34}} = \frac{1}{2 \times \pi \times 100 \times 820 \text{ pF}} = 2 \text{ MHz} \quad (60)$$

2.3.9.2 Voltage Amplifier

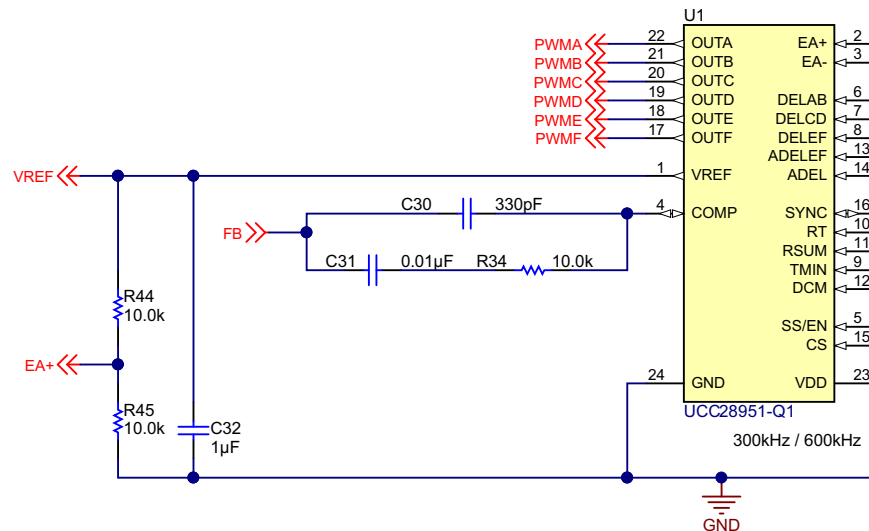
The voltage amplifier reference voltage (pin 2, EA+) is set by a voltage divider (R44 and R45 as the schematic in 图 5 shows) from the internal reference pin (V_{REF}). R44 and R45 are both selected as 10 kΩ to set the reference to 2.5 V. A 1-μF decoupling capacitor is placed close to the V_{REF} pin to filter out the high-frequency noise.

The DC output voltage is set by the voltage divider R29 and R35 + R48. The feedback regulation voltage is set to 2.5 V according to 公式 61.

$$V_{EA-} = V_{OUT} \times \frac{R_{35} + R_{48}}{R_{29} + R_{35} + R_{48}} = 2.5 \text{ V} \quad (61)$$

2.3.9.3 Compensation Network

The compensation network comprises the feedback components C30, C31, and R34, as 图 7 shows. The components must be placed as close as possible to pin 3 and pin 4.



Copyright © 2017, Texas Instruments Incorporated

图 7. Compensation Network

The load impedance (R_{LOAD}) is calculated in 公式 62 as:

$$R_{LOAD} = \frac{V_{OUT}^2}{P_{OUT}} = \frac{12 \text{ V}^2}{400 \text{ W}} = 0.36 \Omega \quad (62)$$

The compensator gain (G_{gain}) in 公式 63 is set to:

$$G_{gain} = \frac{R_{34}}{R_{29}} = \frac{10 \text{ k}}{13.3 \text{ k}} \approx 0.75 \quad (63)$$

The compensation zero in 公式 64 is set at the pole frequency formed by the load and output capacitors:

$$\frac{1}{2 \times \pi \times C_{31} \times R_{34}} = \frac{1}{2 \times \pi \times C_{OUT} \times R_{LOAD}} \quad (64)$$

where,

- C_{OUT} is the total output capacitance,
- R_{LOAD} is the load impedance.

The compensation pole in 公式 65 is set at the ESR frequency of the output capacitors:

$$\frac{1}{2 \times \pi \times C_{30} \times R_{34}} = \frac{1}{2 \times \pi \times C_{OUT} \times ESR} \quad (65)$$

where,

- ESR is the equivalent series resistance of the output capacitor.

C30 and C31 have been selected as 330 pF and 0.01 μ F per the standard values.

2.3.9.4 Soft-Start Capacitor

The UCC28951-Q1 implements a soft-start function to limit the inrush current during start-up. The soft-start time is selected as 5.7 ms. C_{SS} is calculated in 公式 66 as:

$$C_{SS} = \frac{t_{ss} \times 25 \mu A}{V_{EA-} + 0.55} = 48 \text{ nF} \quad (66)$$

2.3.9.5 Adaptive Delay DELAB, DELCD, and ADEL

The UCC28951-Q1 offers two different adaptive delay management techniques which improve the efficiency over a wide load current range:

1. ADEL – This technique sets and optimizes the dead-time control for the primary switches over a wide load current range. The technique also sets the delay between one of the outputs (OUTA or OUTB) going low and the other output going high.
2. ADELEF – This technique sets and optimizes the delay-time control between the primary side switch OUTA or OUTB going low and the secondary side switch OUTF or OUTE going low.

The resistor R51 connected from DELAB pin to GND, along with the resistor divider R41 and R53 connected from CS pin to GND, sets the delay time between the PWM outputs to the MOSFETs at the same bridge, pin OUTA or OUTB going low, and the other output going high, which is represented as T_{ABSET1} or T_{ABSET2} in 图 8.

The CS signal fed into the ADEL pin settles and the dead-time control for the primary side switches dependent of the load current change. The delay time varies reversely proportional to the CS signal amplitude. The delay time gradually increases from T_{ABSET1} , which is measured at $V_{cs} = 1.5 \text{ V}$, to T_{ABSET2} , which is measured at $V_{cs} = 0.2 \text{ V}$. The delay time is fixed, independent of the load, when a fixed voltage is applied to the ADEL pin.

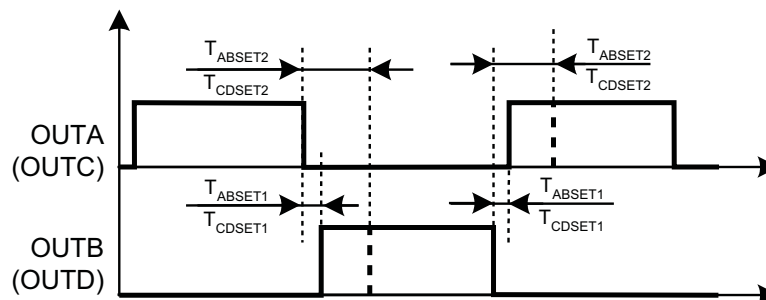


图 8. Delay Definitions Between OUTA and OUTB, OUTC, and OUTD

The turnon delay of primary MOSFETs Q9 (PWM signal OUTB) after Q2 (PWM signal OUTA) is initially set based on the interaction of leakage inductance L_s and the theoretical switch node capacitance. The resonant tank frequency is calculated in 公式 67 as:

$$f_R = \frac{1}{2 \times \pi \times \sqrt{L_S \times (2 \times C_{OSS_QA_AVG})}} = \frac{1}{2 \times \pi \times \sqrt{0.33 \mu\text{H} \times (2 \times 324 \text{ pF})}} = 11 \text{ MHz} \quad (67)$$

The initial t_{ABSET} is calculated in 公式 68 as:

$$t_{\text{ABSET}} = \frac{2.25}{f_{\text{R}} \times 4} = 52 \text{ ns} \quad (68)$$

The coefficient K_{A} defines how significantly the delay time depends on the CS voltage. K_{A} varies from 0, where the ADEL pin is shorted to ground ($R_{53} = 0$) and the delay does not depend on CS voltage, to 1, where ADEL is tied to CS ($R_{41} = 0$). In this design K_{A} is set as shown in the following 公式 69:

$$K_{\text{A}} = \frac{R_{53}}{R_{53} + R_{40}} = 1 \quad (69)$$

Therefore, the resistor from DELAB to GND R_{51} is calculated in 公式 70 as:

$$R_{51} = \frac{T_{\text{ABSET}} \times (0.26 \text{ V} + V_{\text{CS}} \times K_{\text{A}} \times 1.3)}{5} = 13 \text{ k}\Omega \quad (70)$$

where,

- V_{CS} is the voltage seen from pin CS when ZVS is expected to occur.

The turnon delays of OUTC and OUTD are set the same as T_{ABSET} ; therefore, R_{50} is selected as 13 k Ω , as well. The reflected output current is present in the primary of the transformer during the switching transient of MOSFETs Q3 and Q10.

2.3.9.6 Adaptive Delay DELEF, ADELEF

The resistor R_{49} from DELEF pin to GND, along with the resistor divider R_{42} and R_{43} from CS pin to GND, sets the delay time between the PWM outputs to the MOSFETs at the primary side, pin OUTA or OUTB going low, and the related output OUTF or OUTE going low, which is represented as T_{AFSET1} or T_{AFSET2} in 图 9.

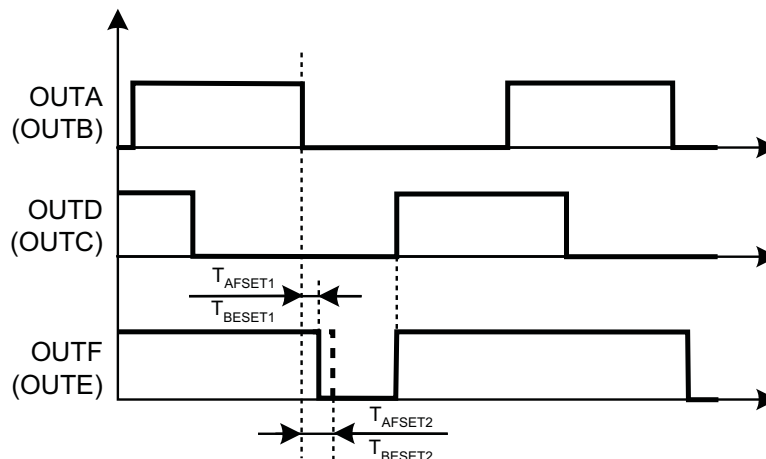


图 9. Delay Definitions Between OUTA and OUTF, OUTB, and OUTE

The turnoff delay of synchronous MOSFET Q1, Q4, and Q5 (PWM signal OUTE) after the turnoff of primary MOSFET Q9 (PWM signal OUTB) is set as 80 ns.

The CS voltage influence of T_{AFSET} has the same implied adaptive delay mechanism as the ADEL circuitry. In this design, the voltage fed into the ADELEF pin is tied to ground through a 10-k resistor; therefore, the coefficient K_{EF} is defined in 公式 71 as:

$$K_{\text{EF}} = \frac{R_{54}}{R_{54} + R_{42}} = 0 \quad (71)$$

The resistor from DELEF to GND R49 is calculated in 公式 72 as:

$$R_{49} = \frac{(T_{AFSET} - 4 \text{ ns}) \times (2.65 \text{ V} - V_{CS} \times K_{EF} \times 1.32)}{5} = 13 \text{ k}\Omega \quad (72)$$

图 10 shows an overview of the PWM switching and output waveforms of the phase-shifted full-bridge converter.

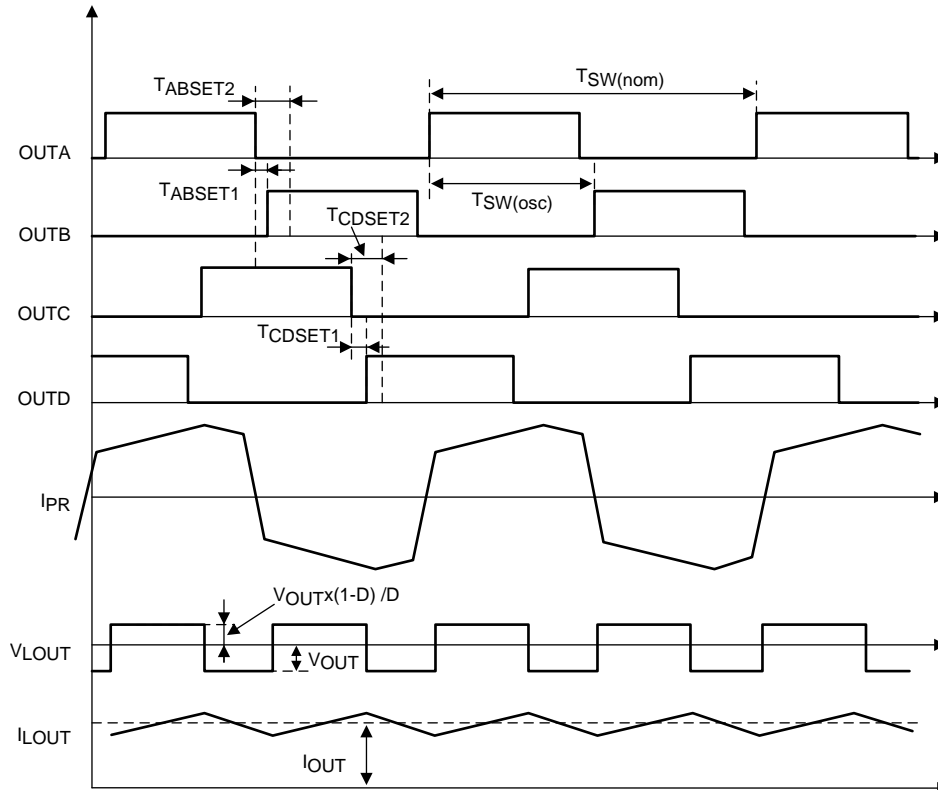


图 10. PWM Control and Output Waveforms of Phase-Shifted Full-Bridge Converter

2.3.9.7 Minimum Pulse (TMIN)

To enable ZVS at a light load, place resistor RTMIN between the TMIN pin to GND to set a fixed minimum pulse width. If the output PWM pulse that the feedback loop demands is shorter than TMIN, the converter enters burst mode where an even number of TMIN pulses are followed by the OFF time dictated by the feedback loop. The TMIN duration must be selected such that it is sufficient for raising the magnetizing current in the power transformer to maintain ZVS. 图 11 shows the typical start-up waveform and burst mode operation of the UCC28951-Q1.

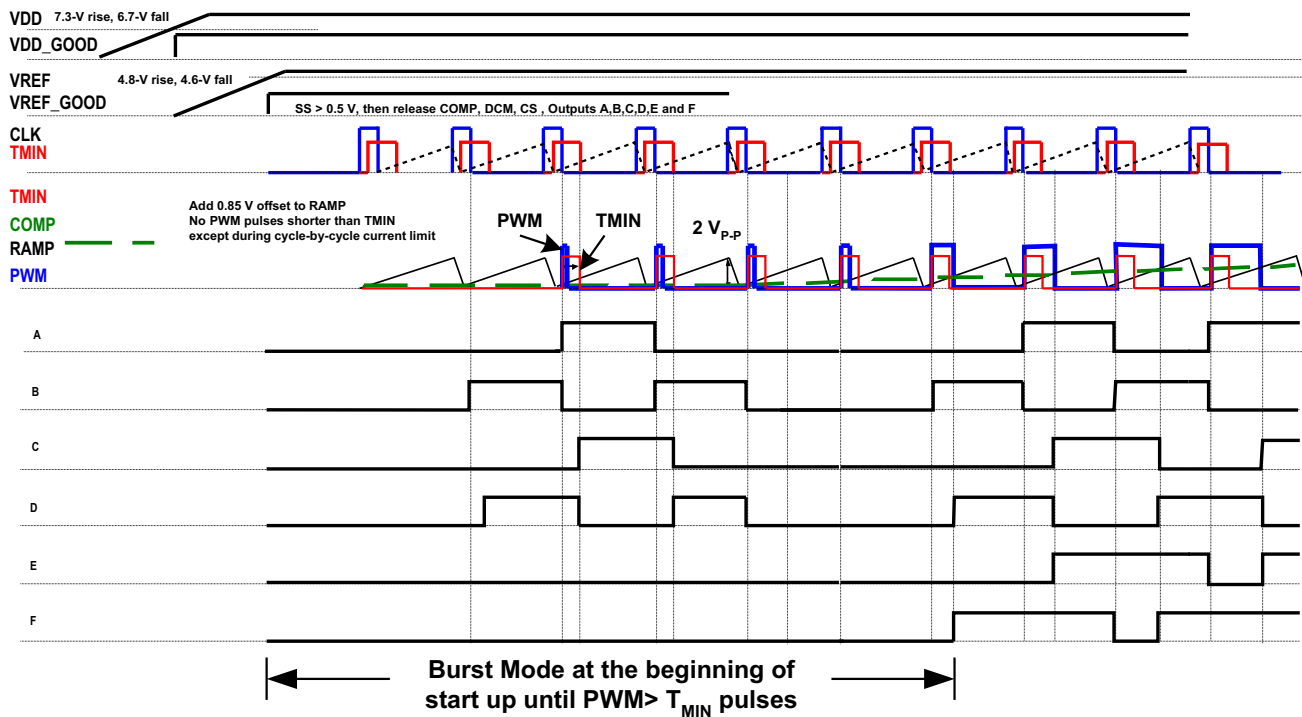


图 11. UCC28951-Q1 Start-Up Waveform and Burst Mode Operation

The minimum ON time for this design is set to 350 ns. R_{TMIN} is calculated in 公式 73 as:

$$R_{TMIN} = \frac{t_{MIN}}{5.92} = 60 \text{ k}\Omega \quad (73)$$

2.3.9.8 Switching Frequency

The external resistor R_T , which is connected from the RT pin to the $VREF$ pin, sets the switching frequency of the UCC28951-Q1. A switching frequency of 300 kHz is selected as a compromise between component size and efficiency. The value of R_T is calculated in 公式 74 as:

$$R_T = \left(\frac{2.5 \times 10^6}{F_{SW}} - 1 \right) \times (V_{REF} - 2.5 \text{ V}) = 18.3 \text{ k}\Omega \quad (74)$$

2.3.9.9 Slope Compensation

Slope compensation is required to prevent a sub-harmonic oscillation in the peak current-mode control [4]. Implement slope compensation by setting R_{SUM} with the following equations. The inductor current-ramp downslope as seen at the CS pin input is calculated in 公式 75 as:

$$m_0 = \frac{V_{OUT}}{L_{OUT}} \times \frac{R_S}{a_1 \times a_2} = \frac{12}{2.1 \mu\text{H}} \times \frac{10}{2.5 \times 100} = 0.23 \frac{\text{V}}{\mu\text{s}} \quad (75)$$

where,

- L_{OUT} is the output inductance,
- R_S is the current sense resistor,
- a_1 is the turns ratio of the power transformer from the primary side to the secondary side (N_p / N_s),
- a_2 is the turns ratio of the current transformer from the secondary side to the primary side (I_p / I_s).

The slope of the additional ramp (m_e), which is added to the CS signal, is obtained by placing the resistor (R_{SUM}) to ground. The value for m_e is calculated in 公式 76 as:

$$m_e = \left(\frac{2.5}{0.5 \times R_{SUM}} \right) \frac{V}{\mu s} \quad (76)$$

The next step is to allow m_e to equalize m_0 ; therefore, R_{SUM} is calculated in 公式 77 as:

$$R_{SUM} = \left(\frac{2.5 \times 2}{0.23} \right) k\Omega = 21.7 k\Omega \quad (77)$$

A 20-k Ω resistor (R47) is chosen.

2.3.9.10 Dynamic SR ON/OFF Control

The voltage at the DCM pin, which is provided by the resistor divider R_{DCMHI} (R39) between the VREF pin and DCM and the R_{DCM} (R52) from the DCM pin to GND. This voltage at the DCM pin sets the percentage of the 2-V current limit threshold for the current sense pin (CS). If the CS pin voltage falls below the DCM pin threshold voltage, then the controller initiates the light-load power-saving mode and shuts down the synchronous rectifiers, OUTE and OUTF. If the CS pin voltage is higher than the DCM pin threshold voltage, then the controller runs in CCM mode.

This design sets the percentage to approximately 10% of the load current. The threshold is calculated in 公式 78 as:

$$V_{RS} = \frac{\left(\frac{P_{OUT} \times 0.15}{V_{OUT}} + \frac{\Delta I_{LOUT}}{2} \right) \times R_S}{a_1 \times a_2} = \frac{\left(\frac{400 \times 0.15}{12} + \frac{6.7 A}{2} \right) \times 8.3 \Omega}{2.5 \times 100} = 0.27 V \quad (78)$$

Set a standard resistor value for R_{DCM} (公式 79):

$$R_{DCM} = 1 k\Omega \quad (79)$$

The resistor value of R_{DCMHI} is calculated in 公式 80 as:

$$R_{DCMHI} = \frac{R_{DCM} \times (V_{REF} - V_{RS})}{V_{RS}} = \frac{1 k \times (5 - 0.27 V)}{0.27 V} = 17.5 k\Omega \quad (80)$$

The resistor value of R_{DCMHI} is finally tuned to be 19.1 k Ω .

3 Getting Started Hardware

3.1 Hardware

图 12 和 图 13 显示 TIDA-01407 的 PCB 板图像，分别从顶部和底部，分别。这些板图像显示了输入和输出连接器、功率变压器、栅极驱动器，以及 RC 缓冲器的 PCB 区域。

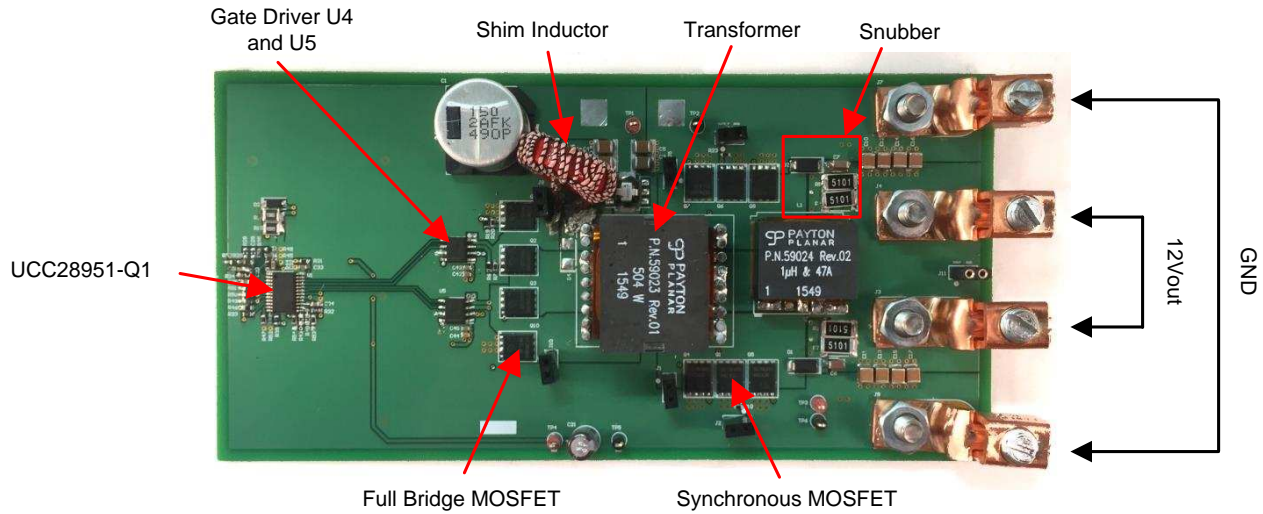


图 12. TIDA-01407 PCB Board—Top Side

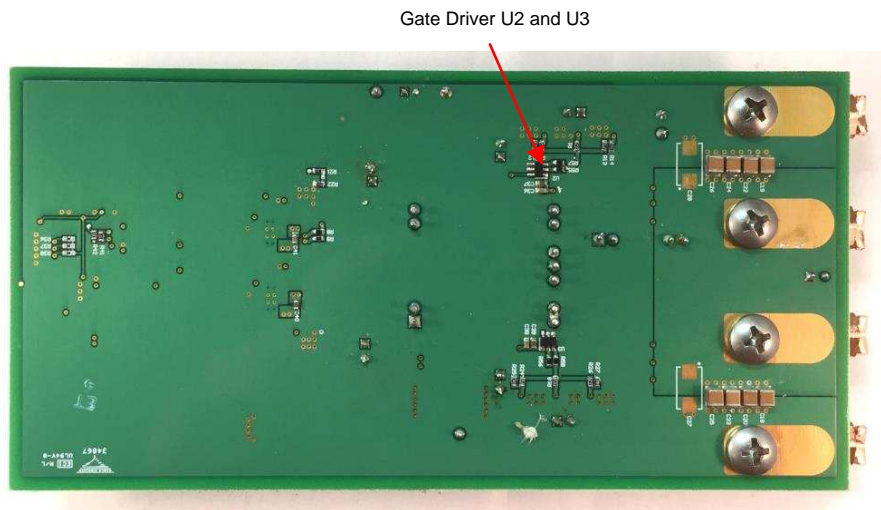


图 13. TIDA-01407 PCB Board—Bottom Side

4 Testing and Results

4.1 Start-Up and Power Down

图 14 shows the start-up waveform of the converter. As the waveform shows, the converter is powered up with a duration of 5.7 ms. 图 15 shows the power down of the converter, where a duration of approximately 370 μ s has been observed.

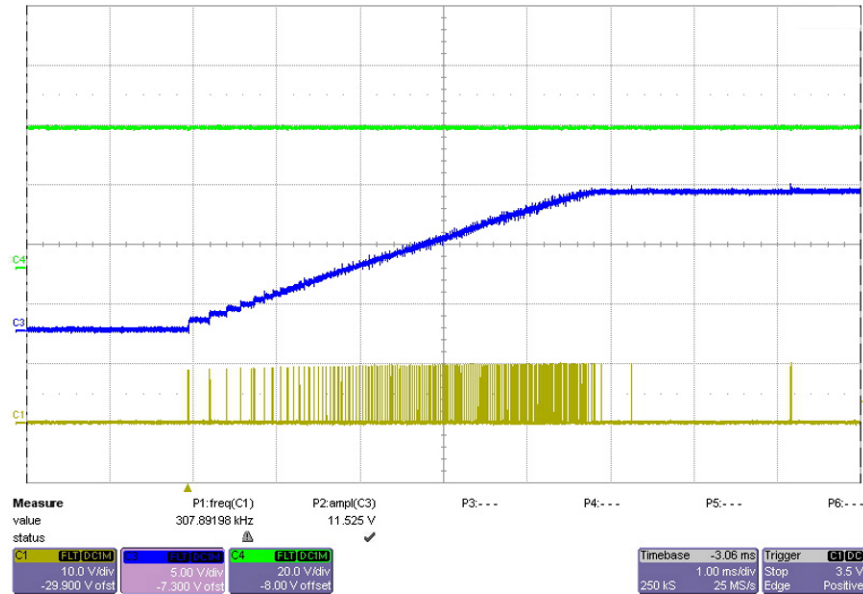


图 14. Start-Up Waveforms of TIDA-01407

注: From top to bottom: CH4 – Input voltage, CH3 – Output voltage, CH1 – Gate drive B

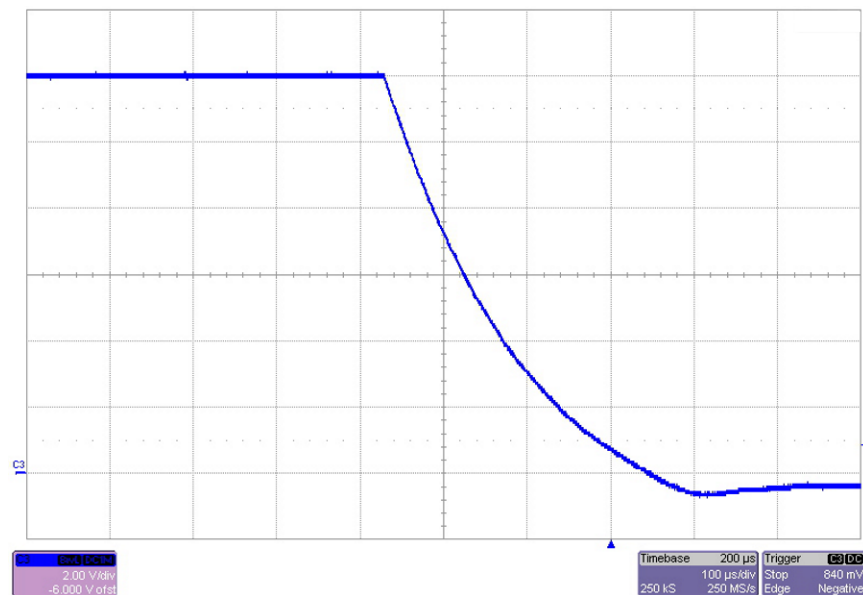


图 15. Power Down Waveform of TIDA-01407

注: CH3: Output voltage

4.2 Output Voltage Ripple

The output voltage ripple of TIDA-01407 is measured under light-load and full-load conditions, respectively. The input voltage is kept constant as 48 V. 图 16, 图 17, and 图 18 show the waveforms. As the waveforms show, less than 20 mV of peak-to-peak ripple voltage is obtained at a 33.3-A full load.

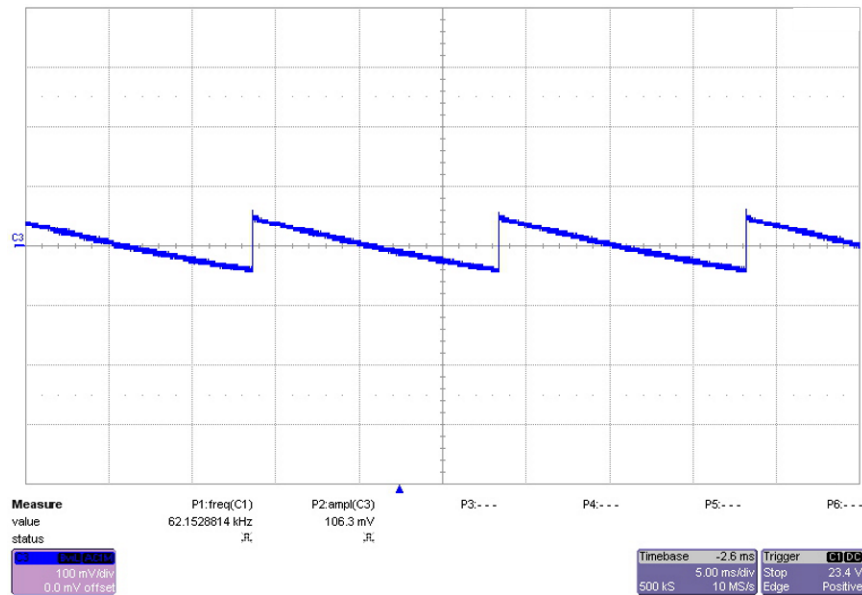


图 16. Output Voltage Ripple of TIDA-01407 With $V_{IN} = 48$ A and No Load

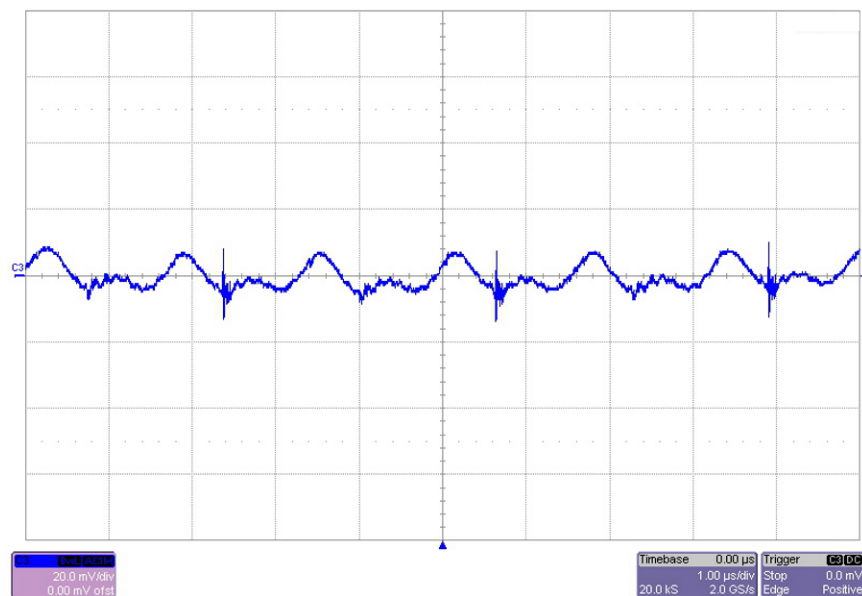


图 17. Output Voltage Ripple of TIDA-01407 With $V_{IN} = 48$ V and $I_{OUT} = 15$ A

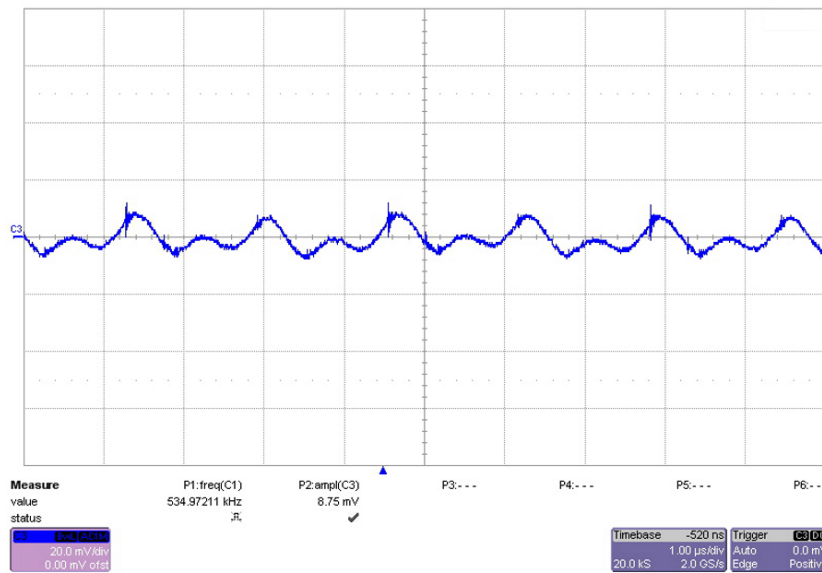


图 18. Output Voltage Ripple of TIDA-01407 With $V_{IN} = 48$ A and $I_{OUT} = 33.3$ A

4.3 Full Bridge Gate Drives and Primary Switch Node Voltages

The gate drive signals versus the switch node voltages of the primary side switches are measured under various load conditions (see 图 19 to 图 24). As the waveforms show, the ZVS resonance occurs earlier when the load current increases.

4.3.1 Under 5-A Load

图 19 and 图 20 show the gate drive signals versus the switch node voltages of the primary side switches under a 5-A load.

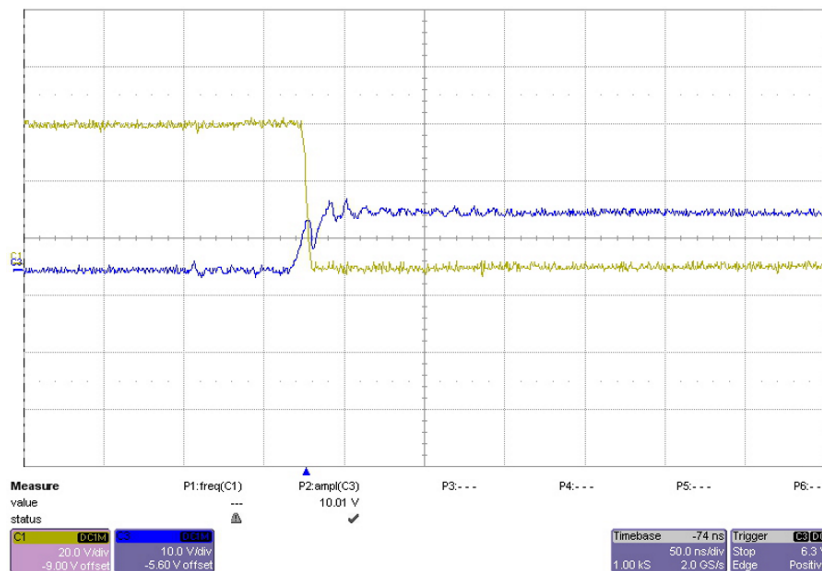


图 19. Switch Node AB (SW_AB) and Gate Drive B

注: From top to bottom: CH1 – Drain-to-emitter voltage of Q9, CH3 – Gate drive voltage of Q9

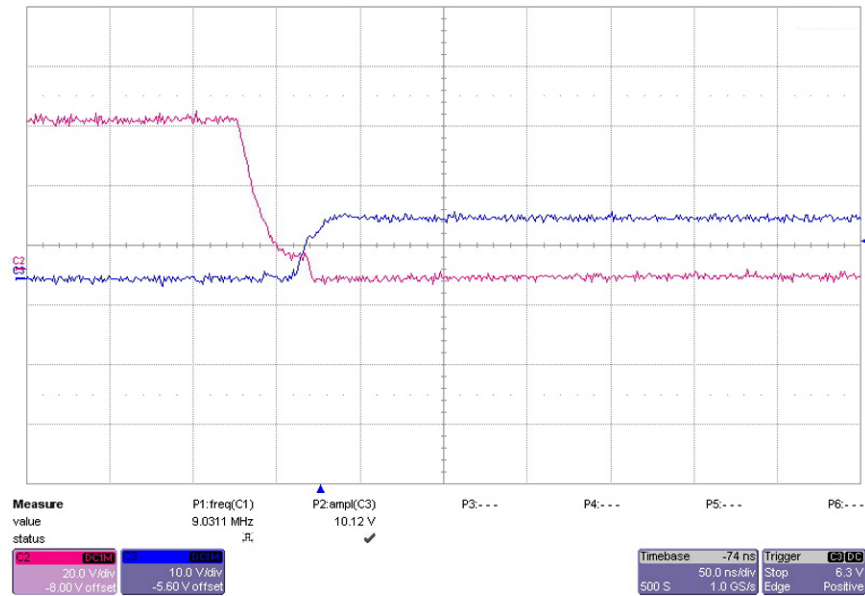


图 20. Switch Node CD (SW_CD) and Gate Drive D

注: From top to bottom: CH2 – Drain-to-emitter voltage of Q10, CH3 – Gate drive voltage of Q10

4.3.2 Under 15-A Load

图 21 和 图 22 显示门极驱动信号与初级侧开关的开关节点电压在 15-A 负载下的关系。

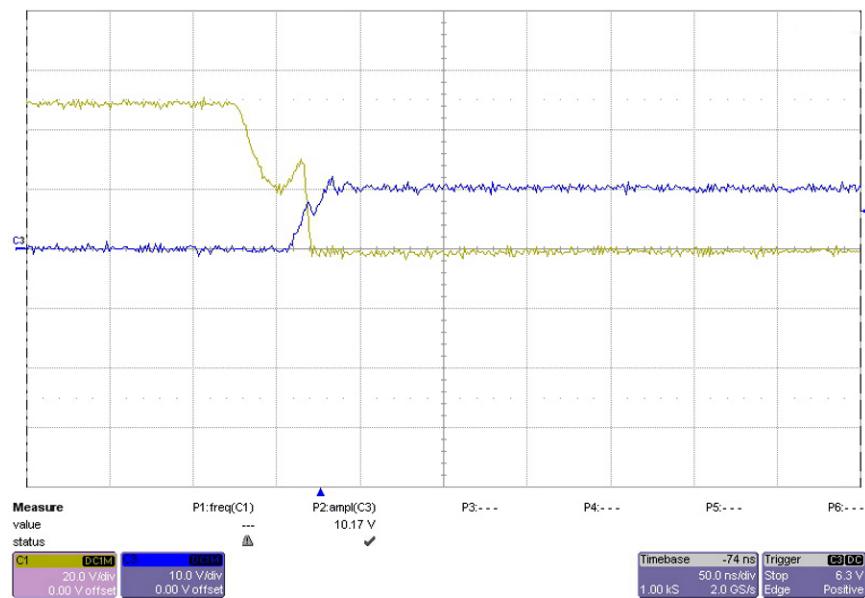


图 21. Switch Node AB (SW_AB) and Gate Drive B

注: From top to bottom: CH1 – Drain-to-emitter voltage of Q9, CH3 – Gate drive voltage of Q9

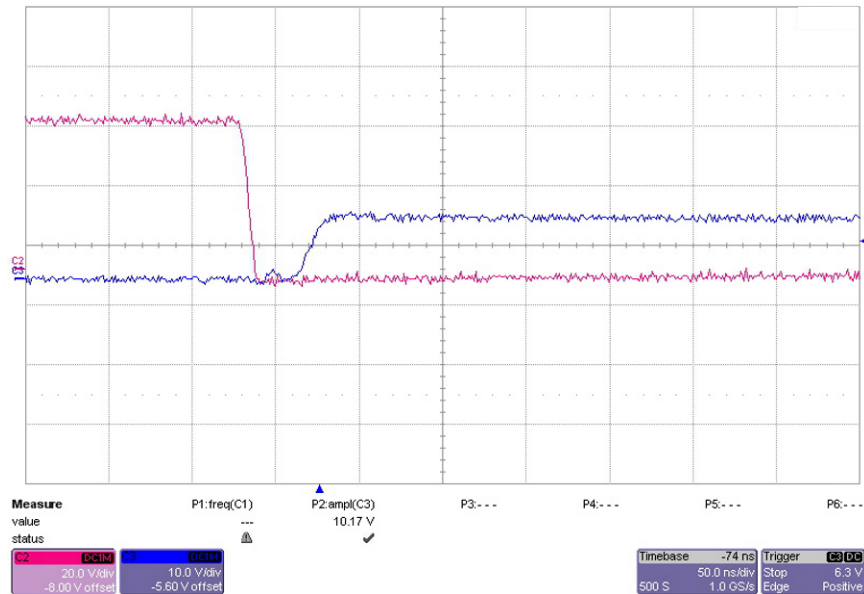


图 22. Switch Node CD (SW_CD) and Gate Drive D

注: From top to bottom: CH2 – Drain-to-emitter voltage of Q10, CH3 – Gate drive voltage of Q10

4.3.3 Under 33.3-A Load

图 23 和 图 24 显示门极驱动信号与初级侧开关的开关节点电压在 33.3-A 负载下的关系。

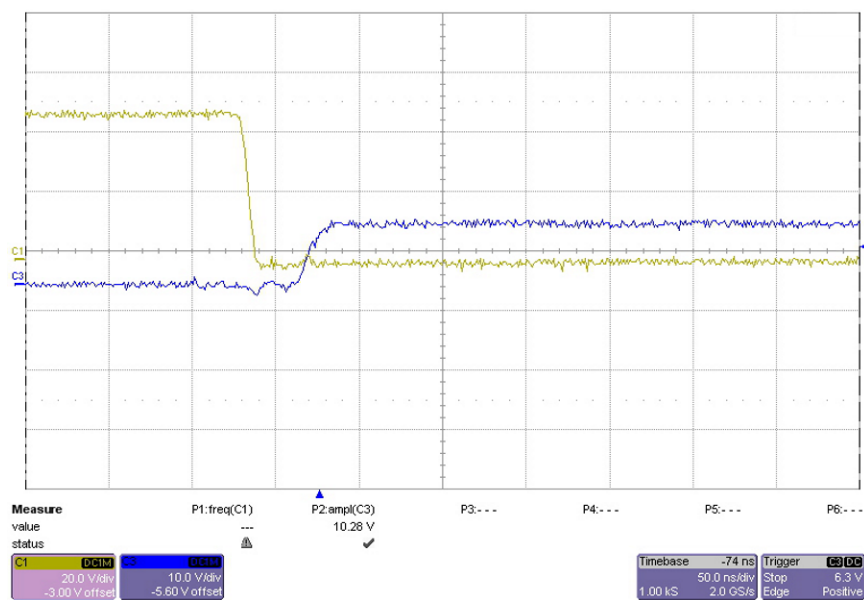


图 23. Switch Node AB (SW_AB) and Gate Drive B

注: From top to bottom: CH1 – Drain-to-emitter voltage of Q9, CH3 – Gate drive voltage of Q9

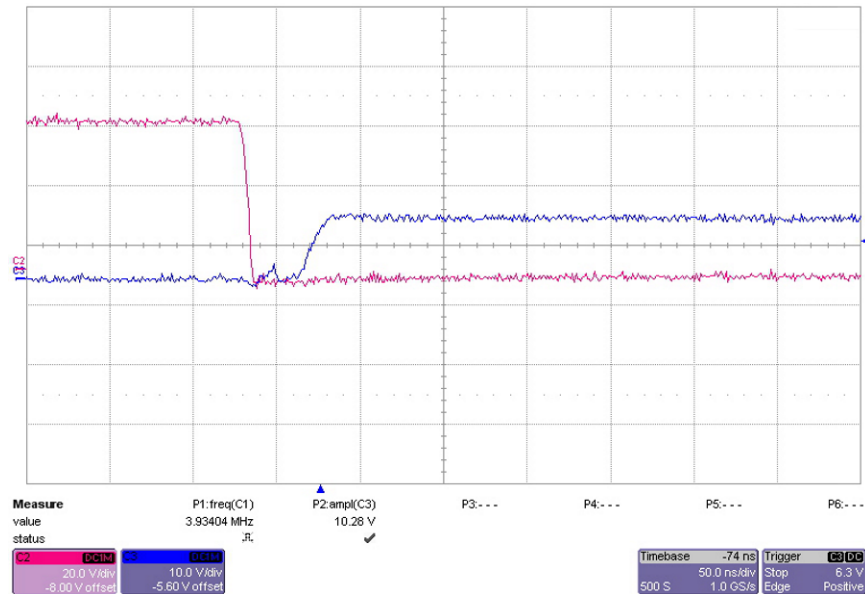


图 24. Switch Node CD (SW_CD) and Gate Drive D

注: From top to bottom: CH2 – Drain-to-emitter voltage of Q10, CH3 – Gate drive voltage of Q10

4.4 Transition of SR From DCM to CCM

The synchronous rectifier (SR) MOSFETs at the secondary side are switched on when the converter runs from discontinuous conduction mode (DCM) into continuous conduction mode (CCM), during which the current flow path changes from the secondary side of the field-effect transistor (FET) body diode to the MOSFET channel. A comparison of 图 25 and 图 26 shows that there is a 730-mV voltage drop across the MOSFET body diode when the converter is running in DCM.

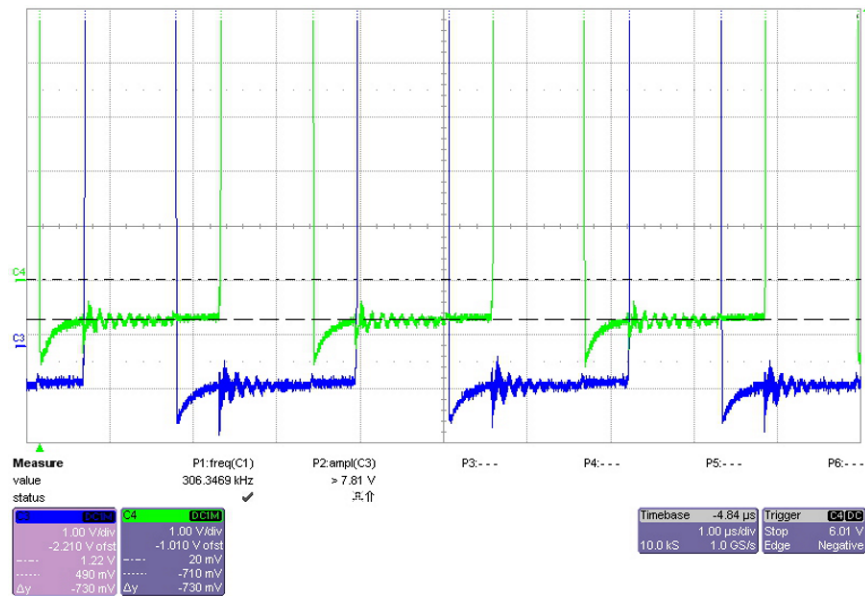


图 25. Switch Node Voltages of Synchronous Rectification MOSFETs When Converter Runs in DCM

注: From top to bottom: CH4 – Switch node voltage of Q6, CH3 – Switch node voltage of Q1

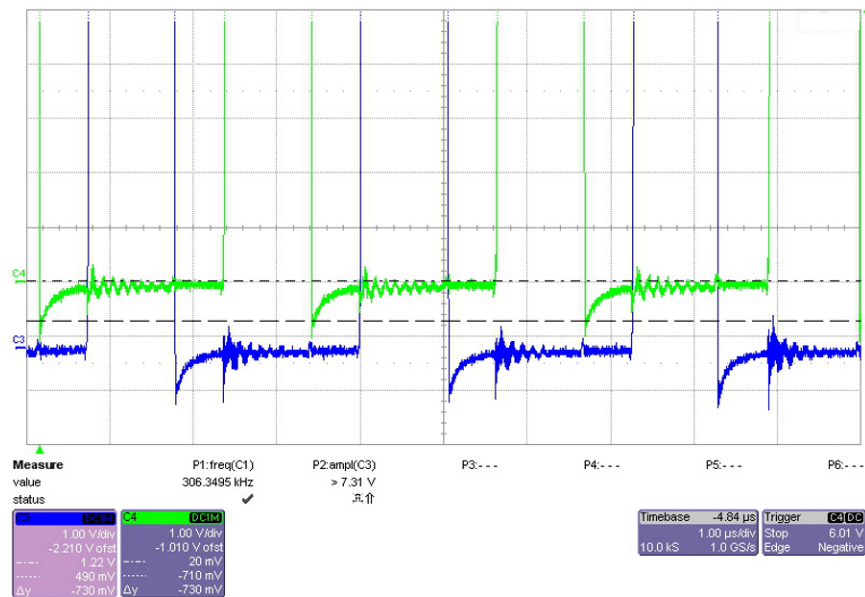
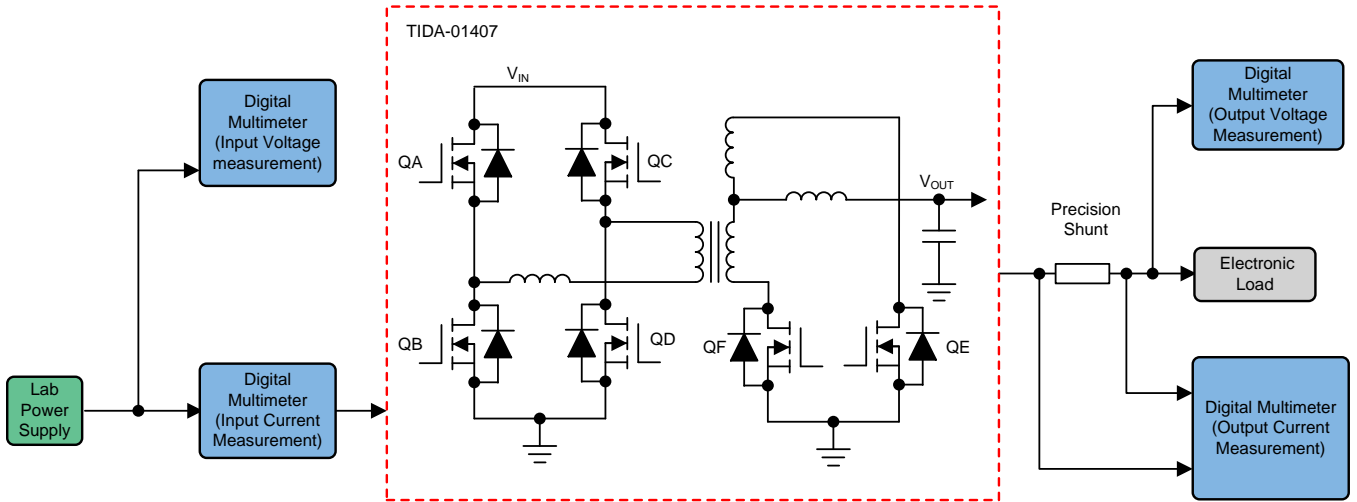


图 26. Switch Node Voltages of Synchronous Rectification MOSFETs When Converter Runs in CCM

注: From top to bottom: CH4 – Switch node voltage of Q6, CH3 – Switch node voltage of Q1

4.5 Efficiency

The efficiency of TIDA-01407 is measured under conditions of varying input voltages. 图 27 shows the measurement setup. Two precision digital multimeters are placed at the input for measuring the input voltage and input current, respectively. One multimeter is placed at the output for measuring the output voltage. The output current is indirectly measured by the voltage drop from a precision shunt resistor.



Copyright © 2017, Texas Instruments Incorporated

图 27. Experiment Setup of Efficiency Measurement

图 28 显示了 TIDA-01407 的测量效率。正如该图所示，在 36-V 输入电压和 22-A 负载下，效率达到峰值 95.5%。

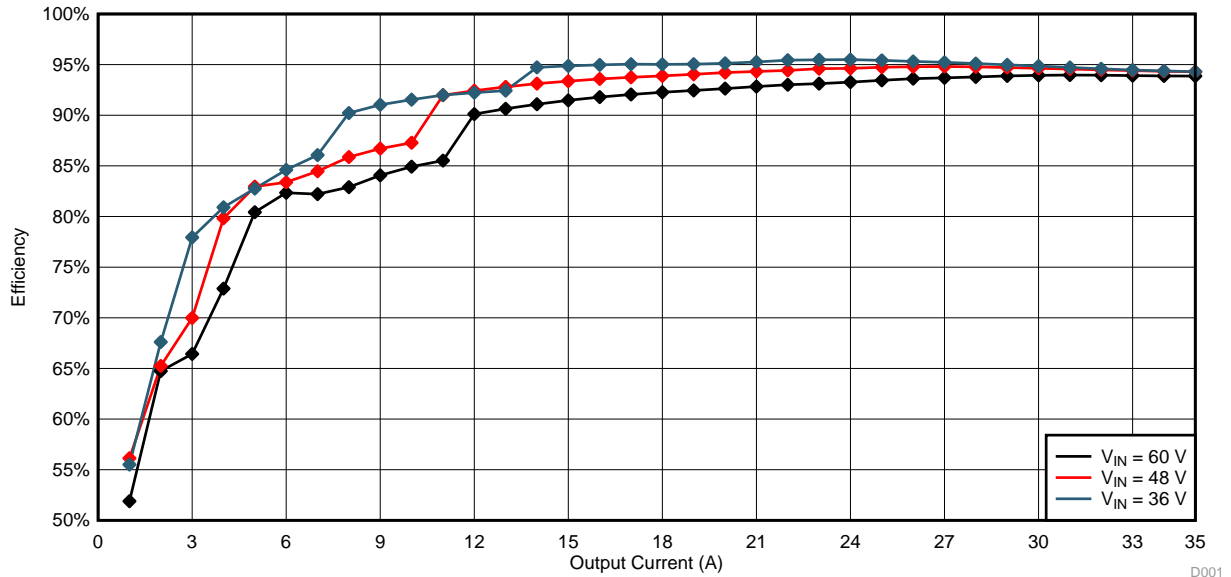


图 28. Measured Efficiency Under Input Voltages of 36 V, 48 V, and 60 V

4.6 Switch Node Waveforms of Synchronous Rectifier

图 29 显示了同步整流器在次级侧的开关节点电压。电阻-电容-二极管 (RCD) 钳位电路必须经过精细调整，以保护 MOSFET 免受过电压。RCD 钳位由二极管 D1、D2；电阻器 R2、R3、R4 和 R5；以及电容器 C6 和 C7 组成。正如该波形所示，振铃峰值被抑制在 61 V 以下。

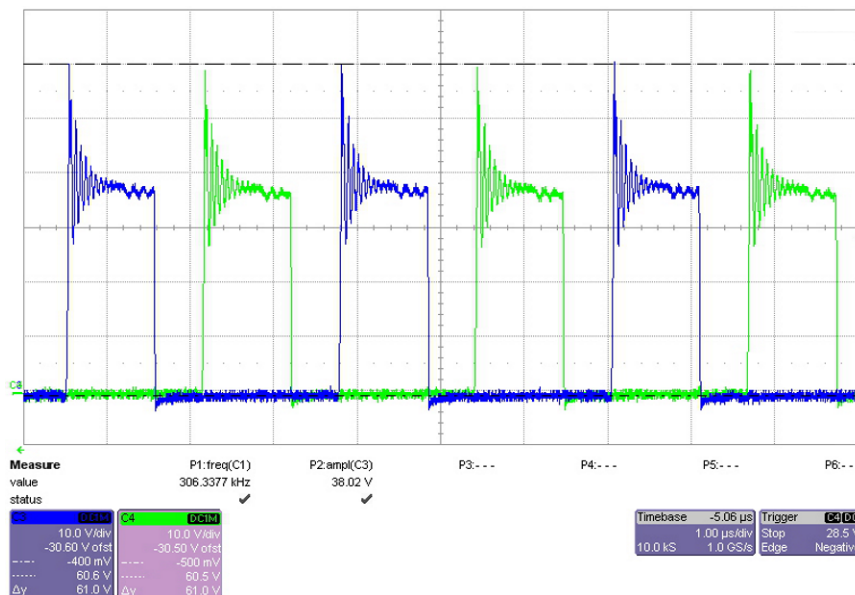


图 29. Switch Node Voltage of Synchronous Rectifier Under $V_{IN} = 48\text{ V}$, $I_{OUT} = 33\text{ A}$

注: From top to bottom: CH3 – Switch node voltage of Q1, CH4 – Switch node voltage of Q6

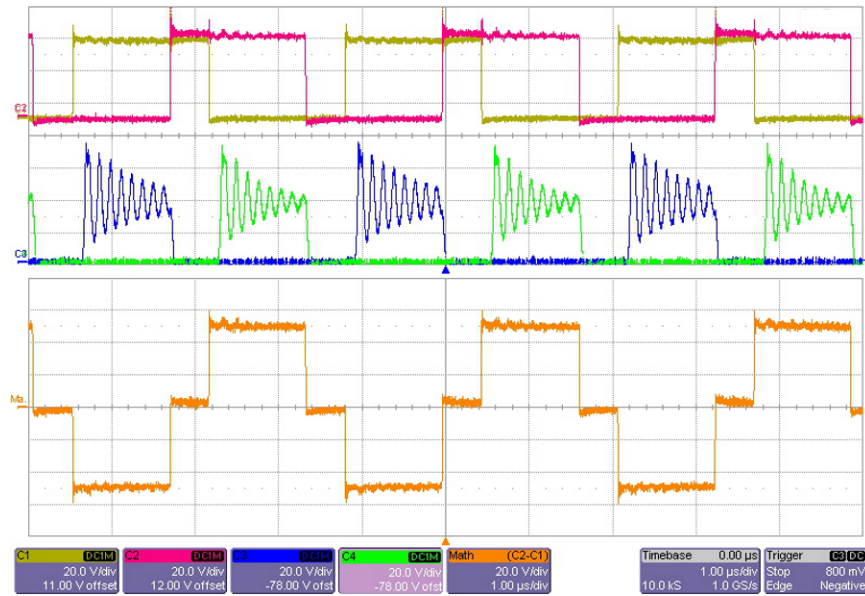


图 30. Switch Node Voltages and Voltage Across Transformer Primary Winding Under $V_{IN} = 48\text{ V}$, $I_{OUT} = 33\text{ A}$

注: From top to bottom: CH1 – Switch node voltage of Q9, CH2 – Switch node voltage of Q10, CH3 – Switch node voltage of Q1, CH4 – Switch node voltage of Q6, Ma – Voltage across transformer primary winding

4.7 Load Regulation

Load regulation measurements show the percent of deviation from the nominal output voltage as a function of output current. The experiment setup is the same as that of the efficiency measurement shown in 图 27. 图 31 shows the measured results with 48-V and 60-V input voltages.

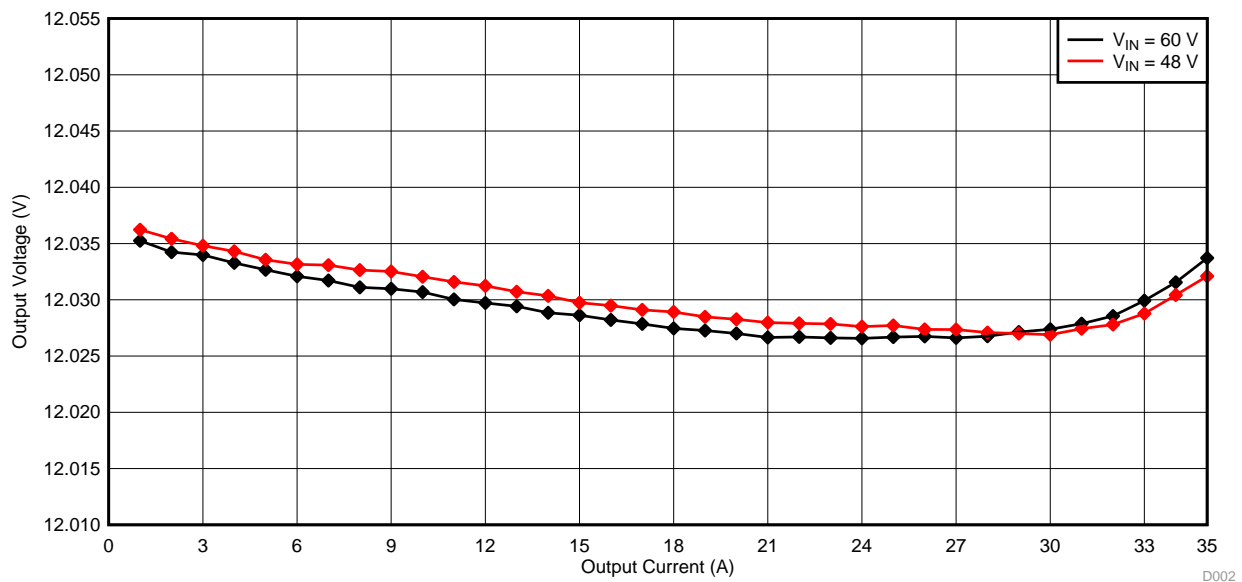


图 31. Load Regulation With $V_{IN} = 48\text{ V}$ and $V_{IN} = 60\text{ V}$

4.8 Load Transient Response

The load transient response presents how well a power supply copes with the changes in the load current demand. 图 32 shows the load transient response of TIDA-01407. The load is switching from 16.5 A to 33 A with a period of 5 ms and a 50% duty cycle. The input voltage is set to 60 V.

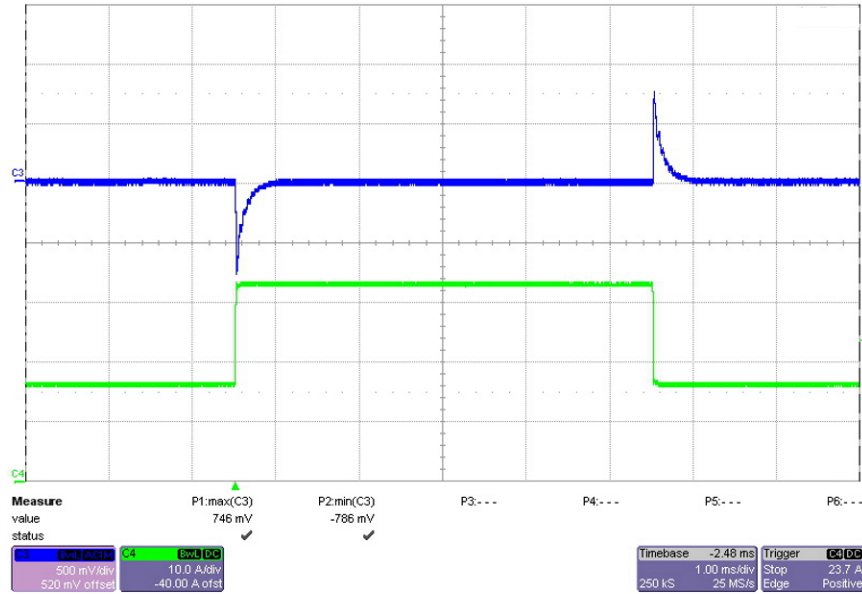


图 32. Load Transient Response With $V_{IN} = 60\text{ V}$ and I_{OUT} Switching Between 33 A and 16.5 A

注: From top to bottom: CH3 – Output voltage ripple, CH4 – Load current

图 33 shows the load transient response when the input voltage is 48 V. The load is switching from 33 A to 16.5 A with a period of 5 ms and a 50% duty cycle.

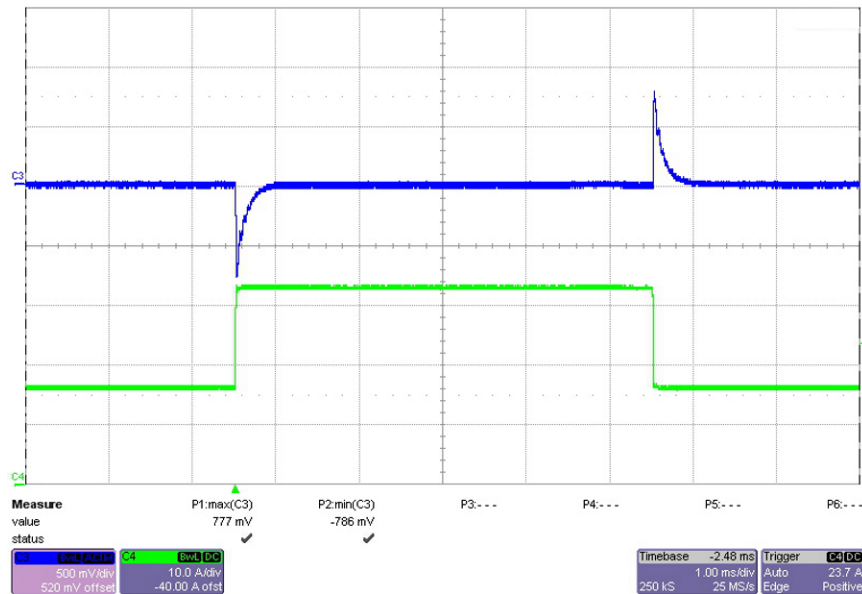


图 33. Load Transient Response With $V_{IN} = 48\text{ V}$ and I_{OUT} Switching Between 33 A and 16.5 A

注: From top to bottom: CH3 – Output voltage ripple, CH4 – Load current

4.9 Thermal Images

The thermal images show the design board measurements under full load conditions. The circuit runs at room temperature for 15 minutes. A 48-V nominal voltage is applied. The converter is loaded with 33 A and the output power is 400 W. 图 34 shows the temperature of the primary side switches Q2, Q9, Q3, and Q10. As the thermal image shows, the peak temperature is 81.2°C.

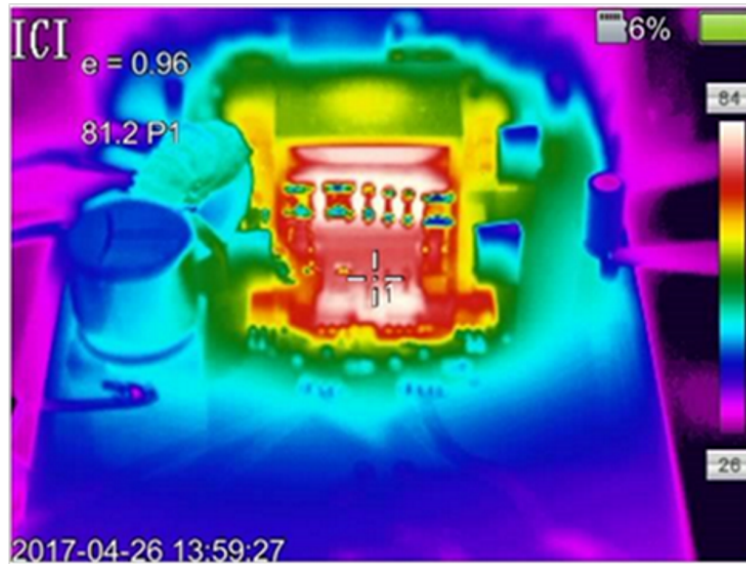


图 34. Thermal Image of Primary Side Switches (Q2, Q9, Q3, and Q10)

注: $V_{IN} = 48\text{ V}$, $P_{OUT} = 400\text{ W}$

图 35 shows the temperature of the power transformer T2. As the thermal image shows, the peak temperature is 63.4°C.

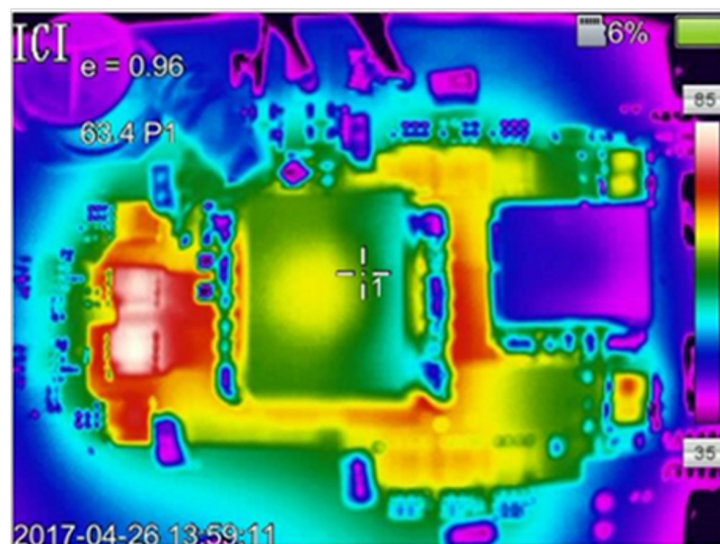


图 35. Thermal Image of Power Transformer T2

注: $V_{IN} = 48\text{ V}$, $P_{OUT} = 400\text{ W}$

图 36 shows the temperature of the synchronous MOSFETs at the secondary side. As the thermal image shows, the peak temperature is 76°C.

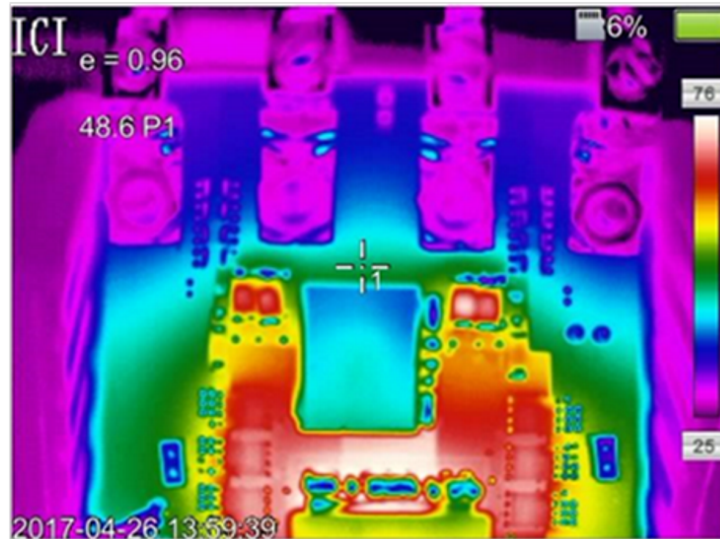


图 36. Thermal Image of Secondary Side Synchronous Rectifier (Q1, Q4, Q5, Q6, Q7, and Q8)

注: $V_{IN} = 48\text{ V}$, $P_{OUT} = 400\text{ W}$

图 37 shows the temperature of the output inductor L1. As the thermal image shows, the peak temperature is 41.7°C.



图 37. Thermal Image of Output Inductor (L1)

注: $V_{IN} = 48\text{ V}$, $P_{OUT} = 400\text{ W}$

4.10 Control Loop Frequency Response

The control loop frequency response represents the stability of the power supply system. The TIDA-01407 loop frequency response is measured under various loads and input voltages, respectively. 图 38 shows the loop frequency response with a 48-V input voltage, 16.5-A load, and 33-A load, respectively. As the graph shows, phase margins of 59.54° and 63.46° are achieved, respectively.

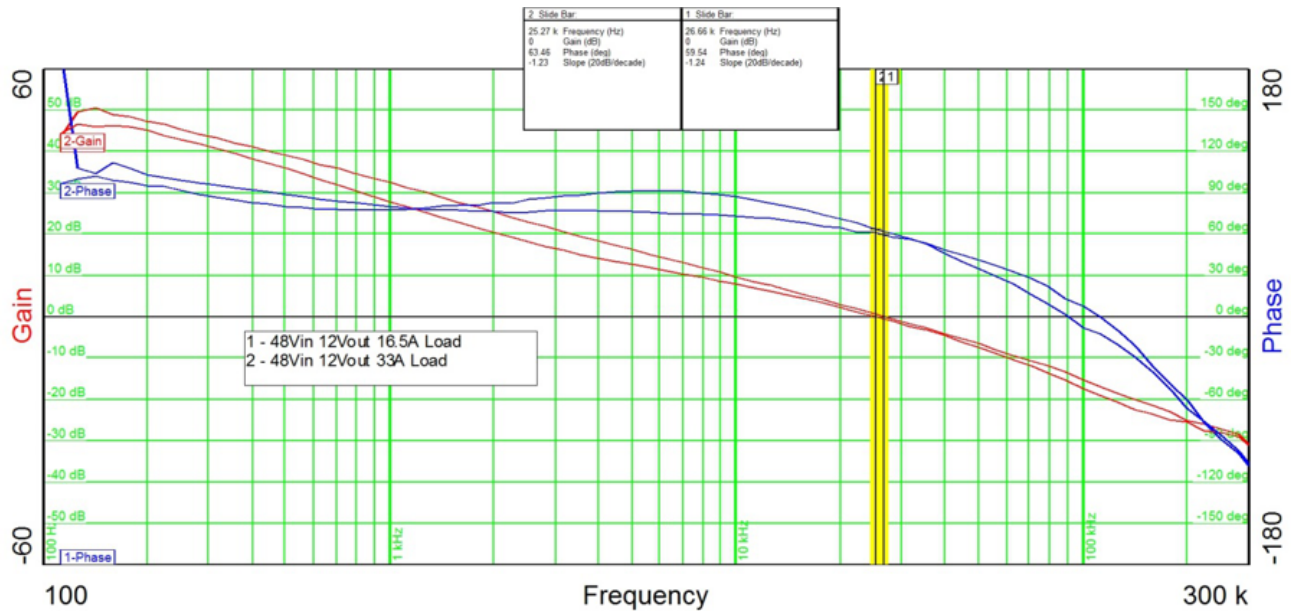


图 38. Loop Frequency Response of TIDA-01407 With $V_{IN} = 48\text{ V}$ and 16.5-A Load and 33-A Load

图 39 shows the loop frequency response with a 60-V input voltage, 16.5-A load, and 33-A load, respectively. As the graph show, phase margins of 57.63° and 58.35° are achieved, respectively.

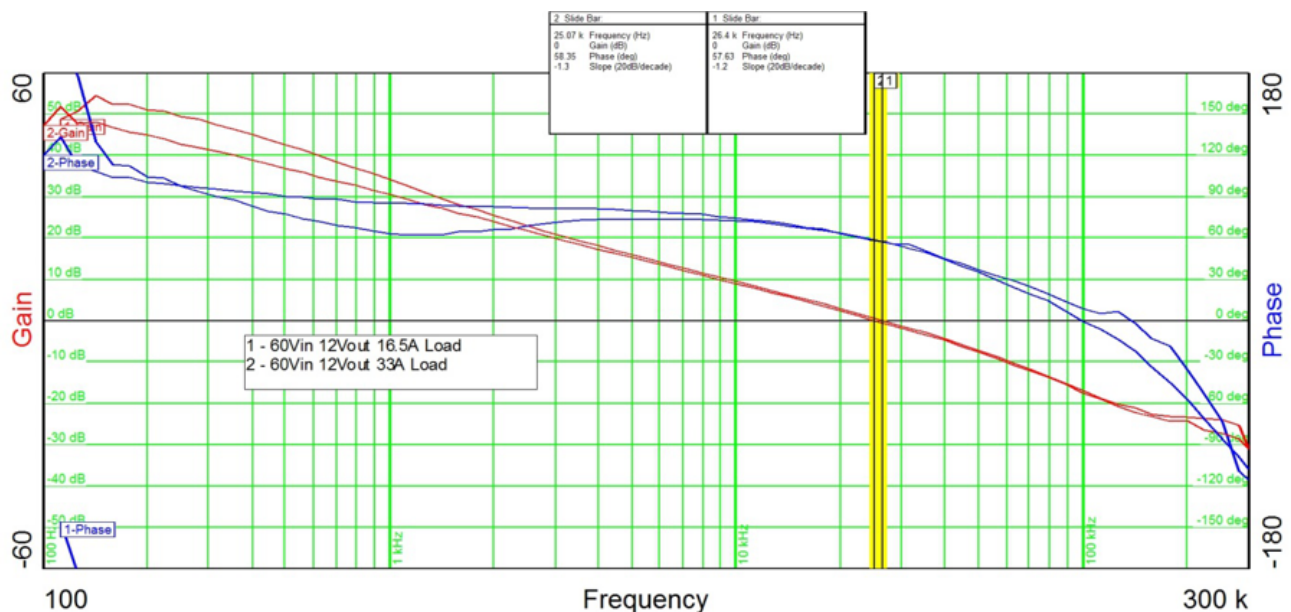


图 39. Loop Frequency Response of TIDA-01407 With $V_{IN} = 60\text{ V}$

5 Design Files

5.1 Schematics

To download the schematics, see the design files at [TIDA-01407](#).

5.2 Bill of Materials

To download the bill of materials (BOM), see the design files at [TIDA-01407](#).

5.3 PCB Layout Recommendations

5.3.1 Layout Prints

To download the layer plots, see the design files at [TIDA-01407](#).

5.3.2 Layout Guidelines

The TIDA-01407 design implements a four-layer PCB. 图 40 lists the board material, copper thickness, and the dielectric distance in between the layers.

	Layer Name	Type	Material	Thickness (mm)	Dielectric Material	Dielectric Constant	Pullback (mm)	Orientation	Coverlay Expansion
	Top Overlay	Overlay							
	Top Solder	Solder Mask/Cov...	Surface Material	0.01016	Solder Resist	3.5			0
	Top Layer	Signal	Copper	0.03556				Top	
	Dielectric1	Dielectric	Core	1.50368	FR-4	4.8			
	Signal Layer 1	Signal	Copper	0.03599				Not Allowed	
	Dielectric 3	Dielectric	Prepreg	0.127		4.2			
	Signal Layer 2	Signal	Copper	0.03599				Not Allowed	
	Dielectric 2	Dielectric	Core	0.254		4.2			
	Bottom Layer	Signal	Copper	0.03556				Bottom	
	Bottom Solder	Solder Mask/Cov...	Surface Material	0.01016	Solder Resist	3.5			0
	Bottom Overlay	Overlay							

图 40. Layer Stack of TIDA-01407

图 41 shows the placement of the input capacitors. TI recommends to place the input capacitors as close as possible to the current transformer T1.

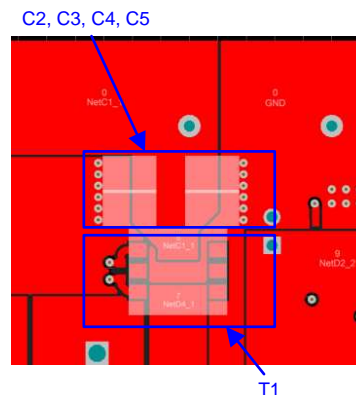


图 41. Placement of Input Capacitors and Current Transformer T1

图 42 shows the Kelvin connection from the current transformer T1 to the UCC29851-Q1 current sense pin. The two traces are kept close and identical to minimize the differential noise crosstalks.

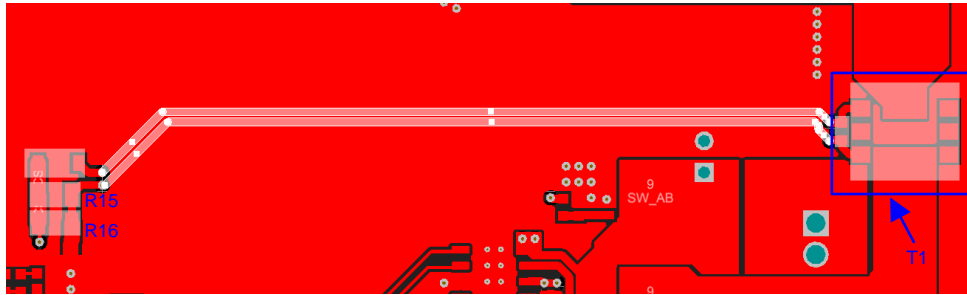


图 42. Placement of RC Filtering Network for Current Sense Pin (PCB Top Side)

图 43 shows the placement of synchronous rectification MOSFETs and the power transformer T2. The synchronous rectification MOSFETs Q1, Q4, Q5, Q6, Q7, and Q8 are placed as close as possible to the transformer secondary winding to minimize the current loop.

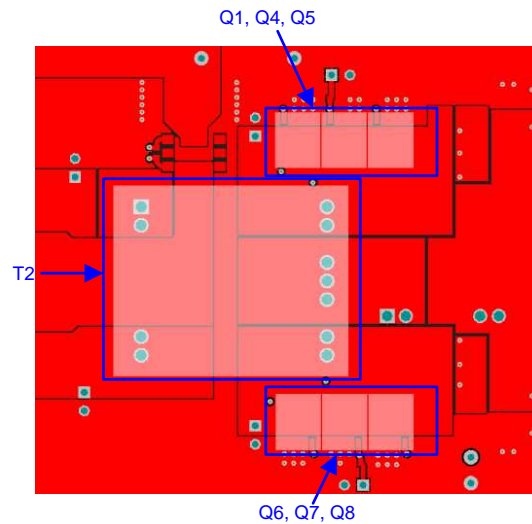


图 43. Synchronous Rectification MOSFETs and Power Transformer T2

图 44 显示了同步整流 MOSFETs 在变压器次级侧以及 RC 箝位电路的放置。箝位电路放置在 MOSFETs 附近以保持电流环路紧凑。

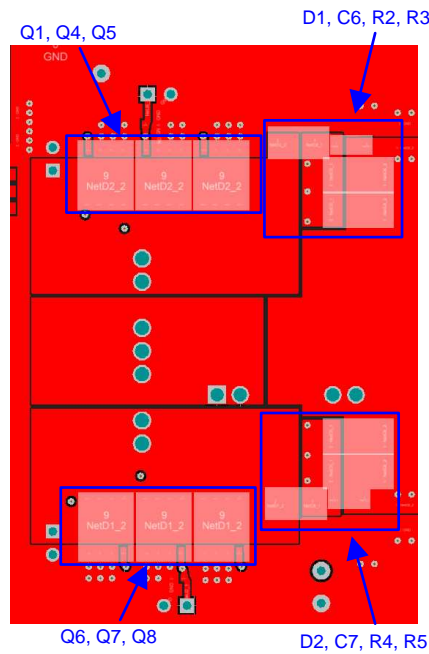


图 44. Placement of Synchronous Rectification MOSFETs and Snubber Circuit

图 45 显示了栅极驱动器和 MOSFETs 在转换器初级侧的放置。这些组件紧密放置以最小化栅极驱动电流环路。栅极驱动电流环路从自举电容器 C40、控制器 IC、栅极电阻、MOSFET Q2 开始，然后回到电容器 C40。

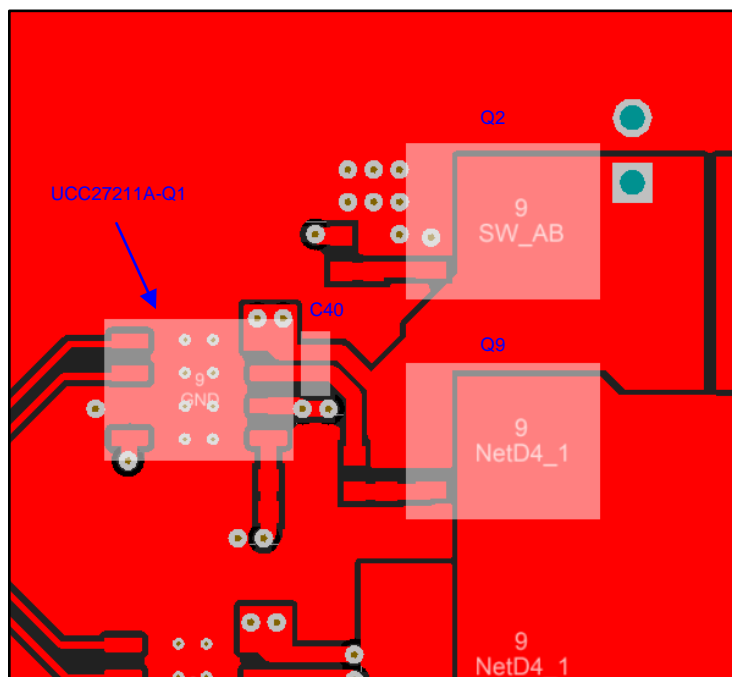


图 45. Placement of Gate Driver and MOSFETs at Converter Primary Side

图 46 shows the placement of the UCC28951-Q1 controller and components surrounding it for configuration. The components are placed as close as possible to the IC to avoid any noise coupling. See the *Layout Guidelines* section in the [UCC28951-Q1 data sheet](#) for more details [5].

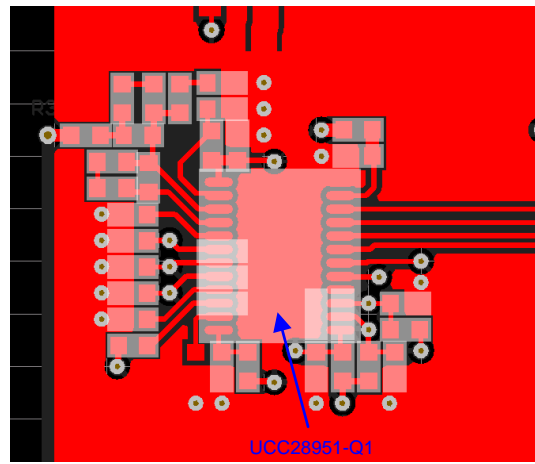


图 46. Placement of UCC28951 Controller and Components for Configuration

图 47 shows the placement of compensation network components. These components are placed on the same side of the controller and as close as possible to the controller.

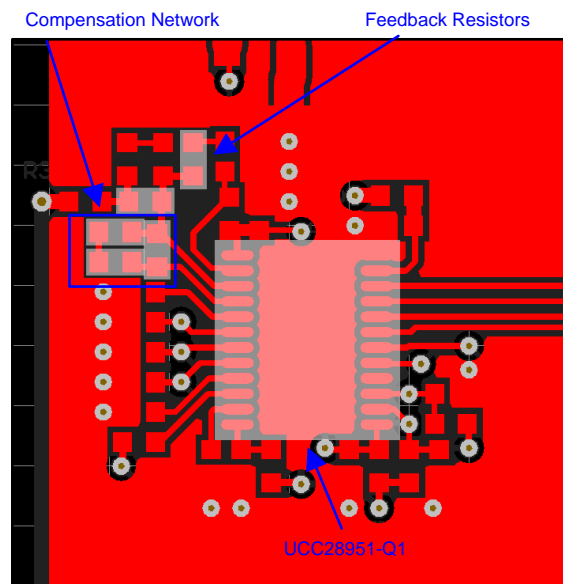


图 47. Placement of Compensation Network

5.4 Altium Project

To download the Altium project files, see the design files at [TIDA-01407](#).

5.5 Gerber Files

To download the Gerber files, see the design files at [TIDA-01407](#).

5.6 Assembly Drawings

To download the assembly drawings, see the design files at [TIDA-01407](#).

6 Related Documentation

1. Texas Instruments, [Automotive Wide \$V_{IN}\$ Front-End Power Reference Design With Cold Crank Operation and Transient Protections](#), TIDA-01179 Reference Design (TIDUC53)
2. Texas Instruments, [A Design Review of a Full-Featured 350-W Offline Power Converter](#), PMP5568 Test Results (TIDU186)
3. Texas Instruments, [UCC28950 600-W Phase-Shifted, Full Bridge Application Report](#), Application Report (SLUA560)
4. Texas Instruments, [Modeling, Analysis and Compensation of the Current-Mode Converter](#), Application Note (SLUA101)
5. Texas Instruments, [UCC28951-Q1 Phase-Shifted Full-Bridge Controller for Wide Input-Voltage Range Applications](#), UCC28951-Q1 Data Sheet (SLUSCK4)

6.1 商标

All trademarks are the property of their respective owners.

7 Terminology

AFE— Analog front end

AEC— Automotive Electronics Council

ESR— Equivalent series resistance

EMI— Electromagnetic interference

EMC— Electromagnetic compatibility

DM— Differential mode

CM— Common mode

DCM— Discontinuous conduction mode

CCM— Continuous conduction mode

UVLO— Undervoltage lockout

MOSFET— Metal-oxide-semiconductor field-effect transistor

CISPR— International Special Committee on Radio Interference

PE— Protective earth

RMS— Root mean square

SR— Synchronous rectifier

BOM— Bill of material

OEM— Original equipment manufacturer

PCB— Printed-circuit board

HEV— Hybrid electric vehicle

EV— Electric vehicle

8 About the Author

XUN GONG is an Automotive Systems Engineer at Texas Instruments, where he is responsible for developing reference design solutions for the automotive segment in HEV/EV Power Train applications. Xun brings to this role expertise in the field of IGBT and SiC (Silicon Carbide) power transistors, EMI and EMC in motor drives, non-isolated and isolated DC-DC converters up to several hundred Watt. Xun achieved his Ph.D. in Electrical Engineering from Delft University of Technology in Delft, Netherlands. Xun Gong won the FirstPrize Paper Award of the IEEE Journal Transactions on Power Electronics in the year of 2014.

RYAN MANACK is the Power Design Services Manager for Automotive, Communications and Enterprise Compute markets. He is responsible for delivering over 350 custom power supply designs a year for global customers in these verticals. Ryan brings to this role expertise in the fields of point of load DC-DC, multiphase DC-DC and isolated DC-DC converters, including half-bridge, full-bridge, and phase-shifted full-bridge converters. He also has five years of experience as a Field Applications Engineer supporting major Consumer Electronic and Enterprise Compute accounts in Silicon Valley. Ryan has a Bachelor's of Science in Electrical Engineering degree from the University of Texas at Austin.

有关 TI 设计信息和资源的重要通知

德州仪器 (TI) 公司提供的技术、应用或其他设计建议、服务或信息，包括但不限于与评估模块有关的参考设计和材料（总称“TI 资源”），旨在帮助设计人员开发整合了 TI 产品的应用；如果您（个人，或如果是代表贵公司，则为贵公司）以任何方式下载、访问或使用了任何特定的 TI 资源，即表示贵方同意仅为该等目标，按照本通知的条款进行使用。

TI 所提供的 TI 资源，并未扩大或以其他方式修改 TI 对 TI 产品的公开适用的质保及质保免责声明；也未导致 TI 承担任何额外的义务或责任。TI 有权对其 TI 资源进行纠正、增强、改进和其他修改。

您理解并同意，在设计应用时应自行实施独立的分析、评价和判断，且应全权负责并确保应用的安全性，以及您的应用（包括应用中使用的 TI 产品）应符合所有适用的法律法规及其他相关要求。您就您的应用声明，您具备制订和实施下列保障措施所需的一切必要专业知识，能够 (1) 预见故障的危险后果，(2) 监视故障及其后果，以及 (3) 降低可能导致危险的故障几率并采取适当措施。您同意，在使用或分发包含 TI 产品的任何应用前，您将彻底测试该等应用和该等应用所用 TI 产品的功能。除特定 TI 资源的公开文档中明确列出的测试外，TI 未进行任何其他测试。

您只有在为开发包含该等 TI 资源所列 TI 产品的应用时，才被授权使用、复制和修改任何相关单项 TI 资源。但并未依据禁止反言原则或其他法律授予您任何 TI 知识产权的任何其他明示或默示的许可，也未授予您 TI 或第三方的任何技术或知识产权的许可，该等产权包括但不限于任何专利权、版权、屏蔽作品权或与使用 TI 产品或服务的任何整合、机器制作、流程相关的其他知识产权。涉及或参考了第三方产品或服务的信息不构成使用此类产品或服务的许可或与其相关的保证或认可。使用 TI 资源可能需要您向第三方获得对该等第三方专利或其他知识产权的许可。

TI 资源系“按原样”提供。TI 兹免除对 TI 资源及其使用作出所有其他明确或默示的保证或陈述，包括但不限于对准确性或完整性、产权保证、无复发故障保证，以及适销性、适合特定用途和不侵犯任何第三方知识产权的任何默认保证。

TI 不负责任何申索，包括但不限于因组合产品所致或与之有关的申索，也不为您辩护或赔偿，即使该等产品组合已列于 TI 资源或其他地方。对因 TI 资源或其使用引起或与之有关的任何实际的、直接的、特殊的、附带的、间接的、惩罚性的、偶发的、从属或惩戒性损害赔偿，不管 TI 是否获悉可能会产生上述损害赔偿，TI 概不负责。

您同意向 TI 及其代表全额赔偿因您不遵守本通知条款和条件而引起的任何损害、费用、损失和/或责任。

本通知适用于 TI 资源。另有其他条款适用于某些类型的材料、TI 产品和服务的使用和采购。这些条款包括但不限于适用于 TI 的半导体产品 (<http://www.ti.com/sc/docs/stdterms.htm>)、[评估模块](http://www.ti.com/sc/docs/sampters.htm)和样品 (<http://www.ti.com/sc/docs/sampters.htm>) 的标准条款。

邮寄地址：上海市浦东新区世纪大道 1568 号中建大厦 32 楼，邮政编码：200122
Copyright © 2017 德州仪器半导体技术（上海）有限公司